

Reviews

Surface phase analysis of catalysts and other disperse materials using electroconductivity: the TVE-curves method

A. A. Dulov,^{a*} L. A. Abramova,^a and S. P. Baranov^b

^a*N. D. Zelinsky Institute of Organic Chemistry, Russian Academy of Sciences,
47 Leninsky prospekt, 117913 Moscow, Russian Federation.*

Fax: +7 (095) 135 5328

^b*P. N. Lebedev Physical Institute, Russian Academy of Sciences,
53 Leninsky prospekt, 117924 Moscow, Russian Federation.*

Fax: +7 (095) 938 2251

The method of thermovacuum electroconductivity (TVE) curves for the analysis of surface phases in disperse systems is described. The theoretical basis of the application of electric measurements for the investigation of the surface of disperse objects is presented. Examples of the use of the TVE-curves method for characterization of diverse catalytic systems and the solving of some problems of heterogeneous catalysis are discussed. The TVE-curves method is an efficient tool for the control of the phase-structural state of the surfaces of objects of a semiconductor type.

Key words: methods for the investigation of catalysts; electroconductivity of disperse materials; the surface of semiconductors.

The development of heterogeneous catalysts with specified properties, one of the main problems of the science of heterogeneous catalysis, requires detailed description of the catalytic surface including data on phase composition and phase transformations. It is well known that the nature of surface phases and the state of interfaces crucially affect the formation and activity of a catalytic system. However, in modern surface science, special attention is paid to studies of local surface sites and structures, whereas no significance is attached to the analysis of surface phases and development of corresponding techniques.¹ One of the new promising approaches to phase analysis of the surface is the use of

electrophysical characteristics. In a series of works, the relation between the electrical parameters of a solid and its bulk and surface phases have been shown,²⁻⁶ and the corresponding techniques for measurement are well developed and fairly simple.⁷

In this review, a method of qualitative analysis of surface phases in disperse materials is described. This is the method of thermovacuum electroconductivity curves (TVE-curves), which is based on the probing of subsurface layers with a direct current when a sample is heated in a vacuum. Special attention is paid to the physical basics of the method; correctness of the use of electric measurements for the analysis of disperse materials is

shown; some approaches to characterization of disperse systems with electroconductivity related to the TVE-curves method are considered briefly, and the place of our method in this row is shown; general basics and potentialities of the method are described; the results of its use for the studying of various catalytic systems with the conductivity of semiconductor type and for the solving of some problems of heterogeneous catalysis are summarized.

Physical basis of the method

The TVE-curves method is based on experimental data obtained by probing of a disperse object with a direct current. Such a method was widely used in the 60s in attempts to develop a general mechanism of redox heterogeneous catalysis on the basis of the electron theory.^{8,9} Although these attempts have not been successful as a whole,¹⁰ the accumulated experimental data and their analysis allowed one to establish a series of important regularities in heterogeneous catalysis.¹¹ In recent works,^{12–17} new correlations between catalytic activity and electrical properties have been discovered. Nevertheless, it is commonly believed now that the high and unstable contact barriers between the granules of a powder and a pronounced sensitivity of the electroconductivity to "the biography" of an object and its surface state rule out, in principle, the possibility of obtaining reproducible and meaningful results of measurements using direct current. However, detailed analysis shows that it is not true.¹⁸ The above-mentioned difficulties of electrical measurements are not of a principle but of an experimental nature, and they can be overcome by the development of an appropriate procedure. The conclusions on the character of information for a disperse system, which are obtained by measurements using direct current, are presented below.

Object and the depth of probing with a direct current

The measurement of electroconductivity with a direct current or alternating low-frequency current (in the kHz region) allows one to investigate surface layers of the grains of a disperse material, because current transfer in such a material generally occurs through the regions of a space charge. The depth of the layer under probing, *viz.*, the radius of the Debye screening, is 10^{-6} – 10^{-4} cm. Unlike the XPS technique, whose data are informative on the average elemental composition of a surface layer, the electroconductivity method is precisely that technique which is sensitive to the phase state of the surface, *viz.*, to the phase composition, distribution, and deficiency (doping) of surface phases. By the character of the information obtained, the electroconductivity differs from other spectroscopic techniques such as IR spectroscopy, which detects no phases but local sites of the surface, *e.g.*, with the aid of adsorbed molecules. On the

other hand, unlike measurements of electroconductivity with an alternative high-frequency current (in MHz region), measurements with a direct current characterize the surface (subcontact) layers, *i.e.*, the regions which are of interest for catalysis but which escape from observation because of shunting at high frequencies.

Barrier effects and the character of the information obtained

The electroconductivity of powders measured with a direct current is limited to the values of barrier (contact) potentials at the intergrain boundaries. However, it characterizes not only these contacts. The electroconductivity with a direct current depends significantly on the bulk properties of a disperse material. Actually, according to calculations performed by Garrett and Brattain¹⁹ as far back as the 50s, intergranular contacts can be considered as a particular case of surface states, and a contact potential can be treated as a contribution (in this case, a predominant one) to the overall surface potential and consequently to the subsurface conductivity measured, which is a characteristic of a subsurface layer depending on the chemical nature of the object. A similar conclusion also follows from the classic works of Slater,²⁰ Petritz,²¹ and others. According to the models developed in these works, the contact potential changes substantially depending on the position of the bulk Fermi level, and consequently changes in the electroconductivity observed contain information about the electronic state of a bulk. However, when one measures the electroconductivity of a powder object, this information is distorted by "noises" of contact potentials. For a single crystal, in the framework of the electron theory of catalysis, one can predict exact correlation between the electroconductivity of a catalyst and its activity.¹¹ As was already mentioned above, in a number of works on powder catalysts, correlations between the electroconductivity and activity, which were predicted for single crystals, were also revealed despite the scatter in the data. This is one more argument in favor of the essential dependence of the electroconductivity of a disperse material on the bulk electronic state of the object.

The theory by Shklovskii²² gives the more general approach to the interpretation of current phenomena in a disperse system. According to this theory, disperse conducting material can be presented as a barrier-disordered system, *i.e.*, as the multitude of contact barriers, different in values, that determine the whole complex of properties expressed in the electroconductivity value measured, σ_{meas} , with the σ_{bul} , σ_{surf} , σ_{cont} , σ_{adm} , $\Delta\sigma_{\text{ads}}$, $\Delta\sigma_{\text{top}}$, *etc.* contributions. Contact barriers (resistances) in a sample may differ by many orders, and for each substance there is a typical function of distribution of contact barriers, whose character depends on both the nature of contacting substances and other conditions: temperature, chemical composition of an atmosphere, *etc.* The overall resistance of a whole system of barriers

and consequently σ_{meas} are also controlled by the value of only one barrier which was named as a key barrier. As a rule, in three-dimensional systems, the value of the key barrier is related to the barrier distribution function as follows: 1/4 to 1/3 fraction of barriers, depending on the average number of neighbors, has the higher conductivity than the key barrier, and the remaining 3/4 to 2/3 fraction has the lower conductivity (Fig. 1, a). The key barrier is statistic, *i.e.*, it is a summarized characteristic of the barrier distribution through conductivities. Due to a huge total number of barriers, the position of the key barrier do not actually undergo random fluctuations and is stable enough to serve as the characteristic of the object under measurement. On the other hand, the position of the key barrier is affected by the properties of all groups of barriers, and consequently, on the basis of its position one can make a conclusion about the state of a whole system. In polydisperse systems, the surface and

contact barriers contribute mainly into the conductivity. When two phases without chemical interaction are mixed, the contact barriers of three types arise in a system: two homophase types of barriers, **AA** and **BB** (with distribution functions typical of pure **A** and **B** phases), and a heterophase type of barriers, **AB**, whose distribution function is unknown beforehand. The overall distribution function of barriers is the sum of these three functions, and their relative contributions depend on the number of contacts of each type. Variation in the component ratio in the mixture results in a change in the position of the key barrier and in the corresponding shift of the key conductivity σ_k (see Fig. 1, b). The existence of such barrier disordering in disperse objects has been confirmed experimentally.²³ The use of the Shklovskii approach for the analysis of experimental data is discussed below (see pp. 260 and 273).

Sensitivity of measurements and boundary conditions

Due to high concentration of intergranular contacts typical of disperse materials, the electroconductivity is very sensitive to a change in the state of an object. The use of a direct current for characterization of these materials allows one to determine an optimum combination of high sensitivity to directed changes in a surface state with the necessary level of statistical stability of the object toward random fluctuations. Figure 2 indicates the advantages mentioned of a polycrystalline object as compared to a single crystal (*cf.* Fig. 2, a and b) as well as those of a direct current in comparison with alternat-

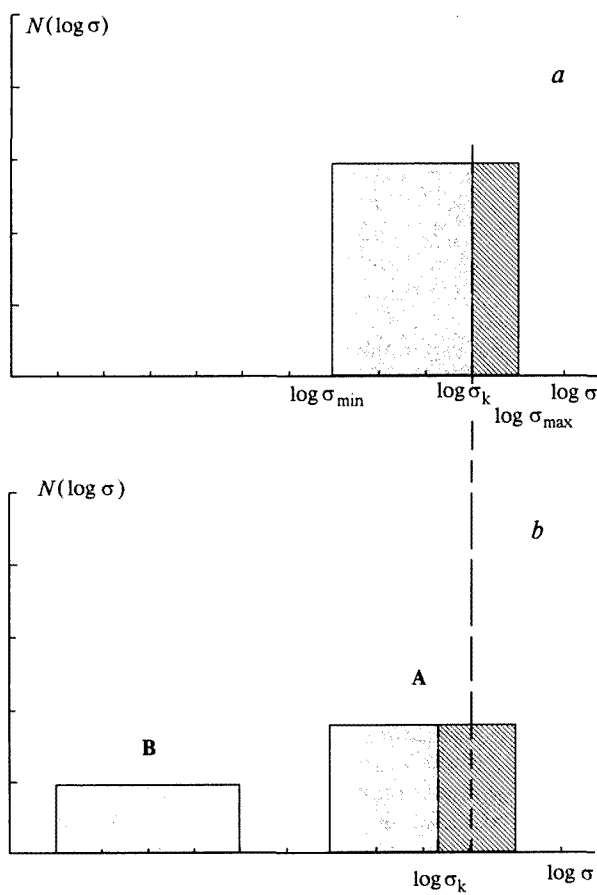


Fig. 1. Barrier distribution function for a polycrystalline material (a) and for a mixture of **A** and **B** polycrystalline materials (b). For the sake of simplicity, the shape of the function was chosen as rectangular; σ_k , a key conductivity. The contribution of the distribution function of the hardly conducting component **B** shifts the value of the key conductivity. Dashed region corresponds to the values in which the fraction of conductivity is higher than that of key conductivity and in both cases is equal to 1/4 of the overall area.

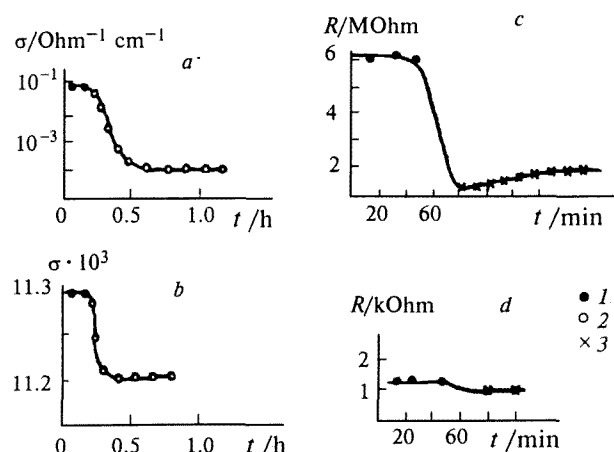


Fig. 2. Sensitivity of the electroconductivity of rutile (a, b)²⁴ and electroresistance of the $\text{ZnO-Cr}_2\text{O}_3$ system (c, d)²⁵ to the adsorption of gases under measurements at various conditions: a, a polycrystalline sample of TiO_2 ; b, TiO_2 monocrystal; c, measurement using a direct current; d, measurement using an alternating current (30 kHz); 1, the starting measurements in a vacuum; 2, oxygen admitting; 3, hydrogen admitting.

ing current (*cf.* Fig. 2, *c* and *d*). However, in friable or too coarsely dispersed powders, intergranular contacts are unstable and undergo such significant fluctuations that the appropriate relation of electroconductivity with bulk properties of a substance is violated. In order for the electroconductivity of a measured object to actually contain the characteristic information about the object that is predicted by theoretical analysis, it is necessary to have a high content and stability of intergranular contacts, under which the electroconductivity is not limited to the number and quality of these contacts. The fact that electroconductivity is independent of voltage (contacts are Ohmic) or of the pressure of the object over a wide range of pressures (from 100 to 5000 kg cm⁻²) can serve as the criterion of fulfillment of the boundary conditions mentioned.

The methodical problem

Thus, the electroconductivity of a polycrystalline (disperse) object measured with a direct current is controlled by contact barriers and through their properties reflects the electronic state of the bulk of the crystallites (grains). When definite boundary conditions are fulfilled, a change in the electroconductivity reflects a change in this state. The measurement of the electroconductivity of polycrystalline materials with a direct current can be considered as a highly sensitive technique for studying processes at the surface and subsurface layers of solids, *e.g.*, adsorption, catalysis, surface and topochemical reactions, and as an essentially possible basis for the method of detecting individual surface phases. For realization of such an opportunity, a technique was necessary that was capable of separating the individual characteristics of the object from the background of "biographical noises." The TVE-curves method solves this problem.

Before starting the description of the TVE-curves method, let us consider briefly some conventional and new applications of electrical measurements for the investigation of catalysts and other disperse materials, because the method of TVE-curves is capable of these same measurements, and comparison with relative approaches will be carried out below (for detailed analysis of the use of electroconductivity for characterization of solids see the review 18).

Some approaches to the investigation of catalysts similar to the TVE-curves method

Percolation dependences of electroconductivity (evaluation of structural-energetic nonuniformity of a catalyst)

Activity and efficiency of a catalytic system are determined not only by its chemical and electronic properties, but also by geometric and topological structure. Geometric factors impose especially strong limitations to

transport characteristics (electro- and thermoelectroconductivity, diffusion), which, consequently, can be used for high-sensitive control of the phase-structural state of a heterogeneous catalyst. Electroconductivity has an advantage as compared to other transport properties, which is important for catalytic studies. It allows one to determine not only the structural peculiarities of an object, *viz.*, the space distribution of microcrystals or small clusters, between which a charge is transferred, but also the energetic parameters of a system. For correct determination of structural peculiarities on the basis of electrical probing, adequate models of both the structure of a system and electroconductivity are necessary, and these models are under development now.²⁶⁻²⁹

Electroconductivity of disperse objects is concerned to so called percolation processes.^{30,31} The percolation phenomenon, which means, in this case, a flow of electric current in a system, is due to the formation of an "infinite", or percolation, cluster, *viz.*, a continuous chain of elements, whose conductivity is higher than a critical (key) value. The possibility of arising of such chain depends on both the number of conducting elements and their space distribution. Minimum concentration of conducting elements, at which they form an infinite cluster, is called by a percolation threshold. The dependence of the electroconductivity on concentration observed experimentally can be characterized by three parameters. The first is the position of the percolation threshold, *i.e.*, the concentration of a conducting phase, at which the conductivity increases sharply due to the arising of infinite conducting cluster. Two other parameters are the slopes of the experimental curve before and after the threshold. The position of the percolation threshold depends on the nature of the distribution of components in the object and can shift from the theoretical value calculated for ideal, statistically uniform distribution. For example, when coarsely dispersed nonconducting elements are "coated" by a highly disperse conducting substance, the formation of continuously conducting contacts proceeds more readily and, as a result, the percolation threshold is lowered. On the contrary, when the nonconducting material covers the surface of conducting elements, the percolation becomes difficult, and the threshold increases (see pp. 272, 273). The slopes of the curve before and after the percolation threshold depend on both the nature of nonuniformity of a system and the ratio of heights of various intergranular barriers, *viz.*, on intergranular interactions. Consequently, on the basis of the position of the percolation threshold and the character of the percolation curve, one can make a conclusion about the distribution of components in the system and the structural peculiarities of the object as well as on the possible interactions in it.

The idea of using the percolation approach for energetic characterization of a surface has been suggested by Shklovskij²² and developed in later works.^{26,27,32} This direction is very perspective for studying catalysts and adsorbents. Thus, in the recent work³³ devoted to the

problem of catalyst poisoning, a developed surface is treated as a fractal, *i.e.*, as the object with intermediate dimensionality (in this case, between two and three) or as a highly branched infinite cluster. Analysis of this object showed that the crushing of a cluster, which distorts the continuous percolation through the whole object, leads to the poisoning of a catalyst. On this basis, the conclusion was drawn that catalysis cannot be treated as a purely local phenomenon, but the collective interactions should be also taken into account. The most important results for the solving the problems of catalysis should be expected from dissemination of the concept of percolation to the structures which are close to real catalysts, *i.e.*, multicomponent systems with interphase interactions. The development of such models is connected with significant difficulties. Now, the parameters of the simplest objects, individual polycrystalline substances and binary systems without chemical interaction, are studied with the aid of computer simulation.

In the framework of the Monte Carlo method, the theoretical models of the electroconductivity of multicomponent powders are proposed.^{28,29} The main parameters of the systems analyzed are the region of a change in conductivities of intergranular barriers, the extent of friability of a powder, and the extent of nonuniformity in the component distribution. It is shown theoretically for binary mechanical **A+B** mixtures that the percolation threshold enhances with a rise in powder friability and is strongly dependent on the extent and nature of nonuniformity in the component distribution (Fig. 3). The lesser mutual incorporation of phases (this corresponds to an increase in W_0 parameter of the model), the weaker is their influence on each other and the sharper is the jump in the conductivity at the percolation threshold. The slopes of the curves in before- and after-threshold regions are due to the ratio of the conductivities of three groups of contact barriers (homophase **AA** and **BB** and heterophase **AB**) and the width of the

corresponding distribution functions. On the basis of these slopes one can judge on the nature of the interaction between the components.

On the basis of these conceptions, one managed to treat the behavior of a series of the mechanical mixtures observed experimentally ($\text{Fe}_3\text{O}_4+\text{MgO}$, $\text{Fe}_3\text{O}_4+\text{NiO}$, $\text{Ni}+\text{ZrO}_2$).^{34,35} An example of this analysis for the mixtures of Fe and Ni oxides prepared by various procedures of components mixing is presented in Fig. 4. Curve 1 describes the experimental data on the electroconductivity of $\text{Fe}_3\text{O}_4+\text{NiO}$ samples prepared by prolonged mixing. It is seen that when the volume fraction of Fe_3O_4 (X) increases from 0 to 0.3, the electroconductivity of the mixtures changes slightly. At $X_c \approx 0.33$, the jump in the conductivity by two orders (a percolation jump) and further monotonous growth to the value typical of Fe_3O_4 are observed. Such a behavior is typical of a statistically uniform mixture, and this is confirmed by a theoretical calculation (curve 3). Curve 2 describes the experimental concentration dependence of conductivity of the mixture of the same oxides prepared by prolonged grinding. The first peculiarity of this curve is the extremely high value of the percolation threshold ($X_c \approx 0.5$) which is typical of either very friable or very nonuniform systems. A significant increase in friability under the formation of the mechanical mixture is unlikely, because the conditions of preparation were standard: the equal dispersion of the starting oxides and the constant pressure of pressing the

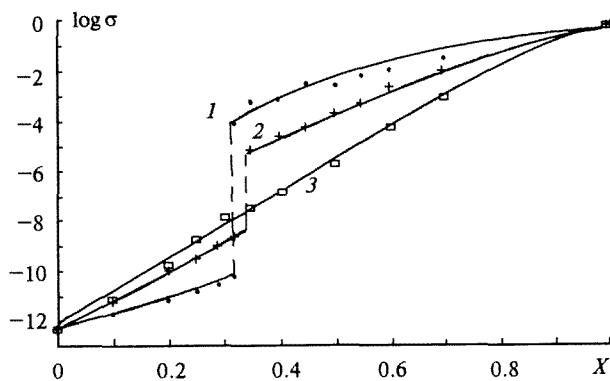


Fig. 3. Dependence of the conductivity of the **A+B** mechanical mixture (X , the fraction of the sites with the highly conducting phase **A**) on the composition with a decrease in the degree of nonuniformity in the distribution of components W_0 : $W_0 = 0.75$ (1); 0.5 (2); 0 (3).

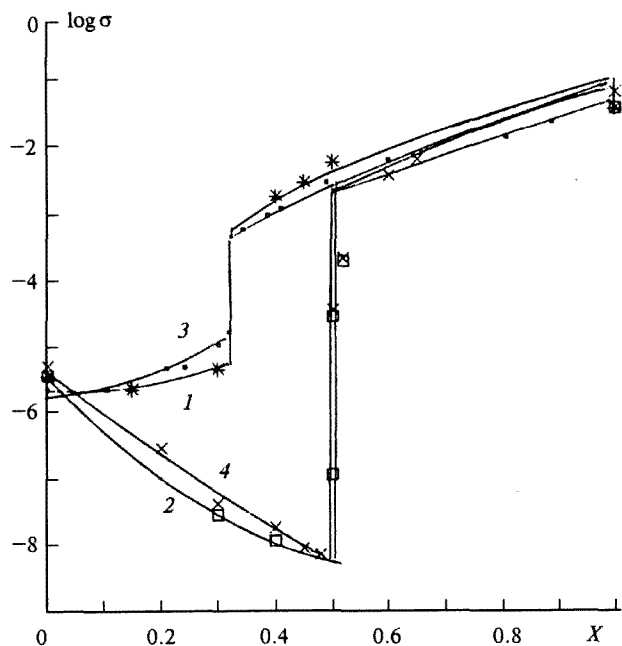


Fig. 4. Electroconductivity of the $\text{NiO}+\text{Fe}_3\text{O}_4$ mechanical mixture (X , the volume fraction of Fe_3O_4) under various modes of component mixing: 1 and 2, the experiment for the mixtures obtained by mixing (1) and grinding (2); 3 and 4, the theoretical calculation for a statistically uniform mixture (3) and for the mixture with deaggregated Fe_3O_4 phases (4).

pellets. More realistic explanation for the high percolation threshold takes into account the nonuniformity of a mixture, in which Fe_3O_4 grains are separated from each other by weakly conducting NiO grains. This distribution can arise as the result of either the incorporation of nonconducting grains into the conducting ones under intense grinding or the breaking of the grains of the conducting NiO phase, which is softer than Fe_3O_4 , and covering of the hard grains of Fe_3O_4 by these moieties. The supposed structure was simulated with the use of the procedure of "deaggregation" of the conducting phase (curve 4). The proximity of curves 2 and 4 points to validity of the model described for the mixture studied.

The second peculiarity of the experimental curve 2 (see Fig. 4) is its negative slope in the before-threshold region. This evidences that as the better conducting component (Fe_3O_4) is added, the conductivity is not improved but becomes weaker. The theoretical analysis^{28,29} shows that such a paradoxical behavior should be observed when arising heterophase contacts (between Fe_3O_4 and NiO granules) conduct still weaker than the starting poorly conducting homophase contacts in NiO . For this system, this fact serves as evidence for the absence of chemical interaction between components. Nickel ferrite, a product of the interaction of Fe_3O_4 with NiO , exhibits high conductivity; therefore, in the case of its formation and substitution of the heterophase contact by nickel ferrite, one could expect a rise in the electroconductivity.

Thus, the computer analysis of the dependence of electroconductivity on concentration and percolation characteristics allows one to establish the structural factors, which determine the observed behavior of an object, and to make a conclusion about the mutual influence of the phases present.

Diagrams "electroconductivity—composition" (control of the formation of phases)

Recording changes in electroconductivity depending on composition is one of the common forms of the use of electrical measurements in the investigation of binary systems.¹⁸ In this way one can reveal the topochemical processes that proceed at various ratios of components in a system and result in the appearance, redistribution, or disappearance of various phases.

This approach should be distinguished from doping with small amounts of additives which was often used for the verification of the electron theory of catalysis.^{8–11} The influence of this doping of semiconductors and catalysts on electroconductivity is studied in detail and well described by the Verwey mechanism. From the topochemical viewpoint, a doping consists of the only process, *viz.*, the formation of solid solutions of substitution.³⁶ According to the Verwey rule of controlled valence,³⁷ the introduction of a cation with a lowered valence into an oxide lattice results in the appearance of

additive positive charge, a hole, and, consequently, to lowering in the energetic boundary of electronic fulfillment, *viz.*, the Fermi level or chemical potential. Correspondingly, the electroconductivity decreases in the case of semiconductor of n-type (electronic) and increases in the case of semiconductor of p-type (hole) as is observed, for example, under the doping of the n-semiconductor ZnO and p-semiconductor NiO with Li^+ ions. The region of the feasibility of the Verwey mechanism is restricted by the limit of the solubility of an additive, *viz.*, usually below 10–15 mol. %. In addition, the conditions of uniform distribution of a solid solution between a surface and a bulk as well as the absence of other compounds in a system should be hold. The most remarkable changes in the conductivity by the Verwey mechanism are observed at the very small content of an admixture, as a rule, below 1 %.

By contrast, diagrams "electroconductivity—composition" discussed in this section are informative in those cases when the significant changes in electrical properties are observed at the concentrations of an additive which exceed substantially the limit of solubility. These changes are mainly due to chemical and structural transformations, therefore, electrical measurements for obtaining the diagrams "electroconductivity—composition" in a wide range of compositions can give information about the interactions between the components and distribution of the phases formed, as it takes place in the case of catalysts.

However, the diagrams "electroconductivity—composition" can be also useful for determining the phase ratios in the case of small amounts of additives. For example, if the direction of changes in the electroconductivity in the range of small additives does not correspond to the Verwey rule, then the reason of a jump in the electroconductivity should be not the formation of solid solutions of substitution, but the arising of a new phase which is distributed in a system in such a manner that is observed already at a very small content. This case corresponds to the conditions of facilitated percolation discussed above (p. 260). Moreover, if the jumps in the electroconductivity under doping with small additives do correspond to the rule of controlled valency, this cannot be obligatory connected with the formation of solid solutions of substitution: the formation of new phases can be also the reason in this case. $\text{NiO}—\text{TiO}_2$ system can serve as an example: the formation of the surface nickel titanate was proved with the TVE-curves method (see the section "Chemical interaction with the formation of a new compound").

All variety of the shapes of experimental diagrams "electroconductivity—composition" can be reduced to three types.¹⁸

The simplest and rare type is a monotonous dependence without extrema. Such a shape of a curve is observed in the systems with unlimited mutual solubility of components which form a continuous row of solid solutions, *viz.*, $\text{CoO}—\text{MgO}$.³⁸ The diagrams for $\text{CeO}_2—$

MgO , Co_3O_4 — Sb_2O_4 , Fe_3O_4 — MgCr_2O_4 systems and the high-temperature NiO — MgO system belong to this type.

Only one extremum is observed in the diagrams of the second type, which indicates the formation of a chemical compound or limited solid solution of components. Such a diagram is obtained for the V_2O_5 — Fe_2O_3 system;³⁹ similar behavior is observed in SnO_2 — Sb_2O_4 , CoO — Al_2O_3 , PbO — TiO_2 , CoO — Mn_3O_4 , NiO — V_2O_5 , and other systems.

Diagrams of the third type are characterized by several extrema that point to the arising of a number of new phases in a system. This is observed for Bi_2O_3 — MoO_3 ,⁴⁰ as well as for Cr_2O_3 — SnO_2 , CuO — Cr_2O_3 , CeO_2 — ZrO_2 , Bi_2O_3 — WO_3 , SnNbO_4 — TiO_2 , etc.

Noteworthy, that in the most of such works, the percolation nature of regularities observed was not taken into account, therefore, the determination of a composition of new phases was not quite correct. In fact, the position of the extremum in a diagram does not coincide with exact composition of the new phase formed but indicates the components ratio, at which the concentration of this phase becomes already sufficient for the formation of infinite conducting cluster. The appearance of a new phase corresponds to somewhat lesser content of the second component than that determined from the position of extremum.

Electroconductivity as the indicator of topochemical transformations

Due to its high sensitivity to changes in the state of a dispersed system and particularly in a phase composition, the electroconductivity proved to be very useful not only for phase control with the aid of "electroconductivity—composition" diagrams, but for successful study of various phase transformations in materials of a semiconductor type. The method of electroconductivity is applicable to the study of virtually all the main types of topochemical processes including the formation of surface phases in various gaseous media (*viz.*, reduction, oxidation, sulfidization, coke formation, etc.), thermal decomposition, topochemical reactions (*viz.*, interphase interaction, exchange, phase transitions of the 1st and 2nd types).^{18,36,41,42} Among objects that are of interest as catalysts, one can point to a number of works on the kinetics and mechanism of the processes of reduction of oxides and oxidation of corresponding metals (Ni, Cu, Fe, Co, etc.) as well as of the processes of partial elimination of lattice oxygen during vacuum heating of oxides which comparatively easily give out a portion of the oxygen (ZnO , CdO , TiO_2 , MoO_3 , SnO_2).¹⁸ Electrical measurements in the study of the reactions of thermolysis of hydroxides, carbonates, oxalates, and other salts, which are precursors of a number of catalytic systems, give valuable information on the mechanisms of genesis of catalysts.^{41,42} The use of the electroconductivity is efficient for observing the very initial stages of interphase interactions, because the electro-

conductivity substantially exceeds in sensitivity both X-ray phase analysis (see p. 270) and thermal analysis for those reactions that start at intergranular contacts. For example, with the use of the electroconductivity it has been shown that the formation of ferrite in the ZnO — Fe_2O_3 system starts 120 °C lower than indicated by the DTA results,⁴³ and the beginning of the interaction between MoO_3 and strontium carbonate to form molybdate phase is registered at 470 °C according to thermal gravimetric data, whereas it occurs already at 100 °C according to the electroconductivity data.⁴⁴

Monitoring of the surface of a catalyst with the use of electroconductivity

Among numerous applications of the method of electroconductivity to the study of solids, "the monitoring by electroconductivity" suggested by Bjorklund and Lundstrom⁴⁵ is the closest to catalytic problems. This approach allows one to use changes in the electroconductivity for observation of any processes at the subsurface region of a catalyst, *viz.*, both topochemical and adsorption—desorption processes. The sensitivity of electroconductivity toward the latter is so high that makes it possible to develop electrical devices for sensors in order to detect traces of gaseous impurities (below 10–13 ppm).⁴⁶

In the strict sense, Bjorklund and Lundstrom only summarized and formulated the idea which actually has long been performed in many studies.¹⁸ This summarized approach proved to be very fruitful. Owing to the use of the electroconductivity as a probe, one can follow various changes in a state of a catalyst at different stages: genesis, performance, deactivation, and regeneration. Unfortunately, the authors⁴⁵ did not develop any common technique, so one should choose a corresponding procedure of electrical measurements for every type of objects.

The studies of a "monitoring" type can also include the observations, for example, for the solid intermediate in a catalytic reaction,⁴⁷ deactivation due to coke formation at the surface,⁴⁸ the periodic changes in a state of the surface of the catalyst in a pulse regime,⁴⁹ as well as above-mentioned works on thermolysis and phase transformation at the initial stages of performance of a catalyst. Monitoring by the electroconductivity was efficient for elucidating the mechanism of the strong metal—support interaction (SMSI).⁵⁰ Thus, for Pt — TiO_2 system studied in detail, the steps of this interaction have been followed and the electronic nature of the effect of the support on the catalytic and adsorption properties of the metal in the case of the SMSI has been shown.^{51–53} The data on electroconductivity is also important for the study of other phenomenon in catalysis which is similar to the SMSI, *viz.*, the strong interaction oxide—support (or oxide—oxide),^{54,55} because in these works, the electroconductivity proves to be one of the most informative tools for investigation (see p. 272).

In the conclusion of the introductory section devoted to various approaches to the use of the electroconductivity for characterization of solids we should stress that the TVE-curves method can be treated partially as a combination and partially as a development of approaches considered. It can be also treated as the modification of monitoring the surface of a catalyst by the electroconductivity and as the efficient method for detecting the topochemical phase transformations in an object as well as improving of the procedures "electroconductivity—composition" and percolation analysis.

Electroconductivity for surface phase analysis (the TVE-curves method)

Prerequisites and analogs. In a series of works,^{2–6} it has been shown that electroconductivity with a direct current and its temperature dependence, when measured in a vacuum or in a gaseous atmosphere, proved to be well reproducible individual characteristics of some substances. However, no works published previously contained the conclusion that such measurements could be the basis of an ingenious technique for phase analysis. The character of the information obtained by probing dispersed materials with a direct current indicates that the electroconductivity can be used for the development of the original method of phase analysis of the surface. Direct evidence for the reality of the development of such an analytical method has been obtained in our previous experiments on the comparison of plots of temperature dependences of the electroconductivity using various catalysts with conductivity of a semiconductor type upon heating in a vacuum.^{56–59}

The method based on electrical measurements which was suitable for conventional phase analysis of the surface, the TVE-curves method, has been finally developed by us to 1979⁶⁰ (see also works 18, 61). It can be categorized to the group of the methods of the type "electroconductivity for surface phase analysis" (ESPA). After the TVE-curves method has already been developed, the reports appeared on the use of some new electrical and electrochemical approaches for the analysis of surface phases: the method of ζ -potential,⁶² the method of the curves of potentiodynamic polarization,⁶³ the method of the chronopotentiometric curves,⁶⁴ the method of the point of zero charge,⁶⁵ as well as the topographic description of the surface with the use of work function in the method of scanning tunnel microscopy (STM).⁶⁶ Each approach including ours gives the intrinsic specific picture of a phase state of the surface and does not duplicate the others.

The principle. The use of the electroconductivity for phase analysis is impossible without a measurement technique which could allow one to separate characteristic information about a dispersed object from a "biographic noise" in the data obtained with a direct current. The scattering in the values of the electroconductivity for various samples of the same substance is too great that

these values are not suitable as individual characteristics of an object. For example, the values of the electroconductivity of NiO , CuO , and ZnO reported by various authors are represented as the vertical lines which are overlapped (Fig. 5, *a*). However, the averaged values of the electroconductivity for each oxide shown by arrows differ from each other. In other words, statistically reliable differences in the electroconductivity of individual oxides occur. Consequently, a possible method to reveal the individual information about an object from the electrical data could be a thorough standardization of the procedures of preparation and characterization of objects under comparison. But this way is extremely laborious and hardly practicable.

We suggested another principle for the solving of the methodical problem: to make the "scanning" of superimposed segments (see Fig. 5, *a*) through the temperature of a measurement. As is shown in Fig. 5, *b*, for each oxide its own band, a sort of a "temperature spectrum of electroconductivity" is obtained. These bands differ significantly from each other in a shape and position, therefore, they can be successfully used for the phase analysis upon combined presence of several oxides.

When the electrical characteristics are obtained by this procedure, the differences between objects become noticeable, because with a gradual rise in a temperature of heating *in vacuo*, two additional processes appear,

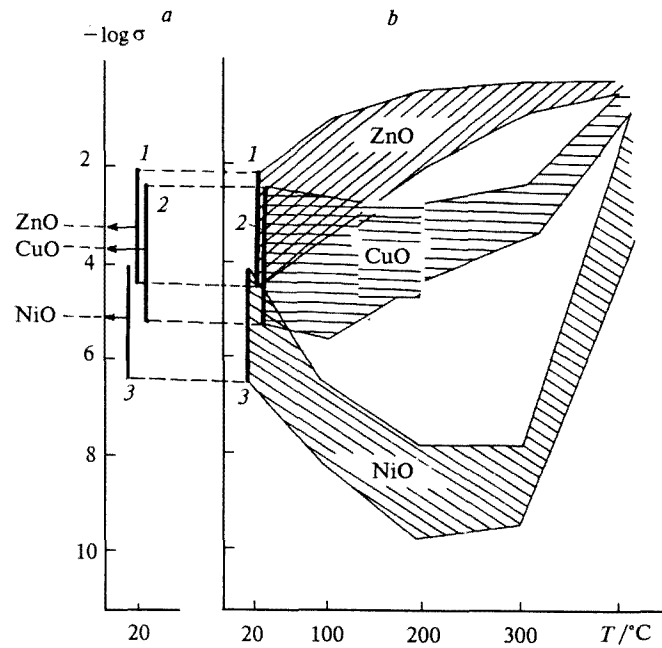


Fig. 5. Scheme of obtaining the characteristic bands of electroconductivity by a "temperature scanning" of the lines of scattering: *a*, the segments which represent the scattering of the results at the same temperature of measurement for ZnO (1), CuO (2), and NiO (3) oxides; *b*, the "scanning" of the same lines of scattering with the measurement of electroconductivity during a rise in temperature of heating in a vacuum.

which variously affect the electroconductivity of different objects. The first process is a desorption. It reflects mainly the desorption of oxygen and determine a shape of the left, low-temperature fraction of the band. In this case, the electroconductivity of p-semiconductors with high sensor sensitivity (NiO) falls; the electroconductivity of less sensitive p-semiconductors (CuO) changes slightly and that of n-semiconductors (ZnO), by contrast, increases. The second process which occurs when a sample is heated *in vacuo*, is of a topochemical nature. It affects a shape of the right, high-temperature fraction of the band: with a rise in a temperature, the deficiency of a lattice increases and oxygen ions are removed from anionic sites. In NiO, this process starts at ~ 250 °C; at 350–400 °C the reduction of NiO results in the appearance of metallic disseminations. In other oxides, topochemical distortions of a lattice are observed at other temperatures, and the electroconductivity changes in another way.

Thus, the main peculiarity of the method described consists in that a run of irreversible changes in the electroconductivity rather than merely the value of electroconductivity at a definite temperature is recorded, when the object is heated in a vacuum. In this way, it is possible to use purposefully a high sensitivity of the electrical measurements to changes in a state of the object which is usually a source of noncontrolled scattering in experimental values. The shifts in electroconductivity that occur in a specified regime of vacuum heating are sensitive to the nature of the object and overcome significantly a random scattering of electric values at each temperature. Therefore, the plots obtained, *viz.*, the thermovacuum electroconductivity curves, or the TVE-curves, have a shape typical of this individual substance independent of the "biography" of a sample, and consequently they can be used as the standards in the phase analysis.

The specific shape of these plots is due to the dependence of electroconductivity on the following main factors, whose relative contribution is determined by the chemical nature of an object and is different in various temperature regions:

— a reversible increase in electroconductivity with rise in temperature according to the Arrhenius law, which is typical of semiconductors and for various substances covers a wide range of values of the activation energy of conductivity E_σ , from ~ 0 to several electron volts;

— a decrease in the coverage of the surface as a result of desorption of gases and vapors (oxygen, water), whose effect is greatest on heating to 200–300 °C. Changes in the electroconductivity caused by this effect are different not only over a range of values, but are also opposite in sign (for n- and p-semiconductors);

— reductive processes in a vacuum which change the nature and the extent of deficiency of a lattice. For example, in the case of an oxide, it is the removal of lattice oxygen resulting in the formation of strongly

deficient or quasi-metallic structures, which is the most noticeable in the range of 300–400 °C (depending on the lattice energy);

— other processes in a lattice: decomposition of residual hydroxides and carbonates, structurization, crystallization, *etc.* These processes occur if the temperature of thermal pretreatment is insufficiently high (for example, in the *in situ* regime).

Noteworthy that at present the computer simulation of the processes mentioned, which determine a character of the TVE-curves in various temperature ranges, is carried out with the use of the program packet developed by us.^{28,29} This will permit to evaluate quantitatively the contribution of different components into the experimental σ_{meas} value; as a result, the TVE-curves method will obtain a deeper physical ground, and the opportunity will appear to judge more thoroughly about the state and changes in an object.

The procedure. The measurements of electroconductivity are carried out in a vacuum cell (10^{-4} – 10^{-5} Torr) with the use of a set of ohmmeters and teraohmometers (*viz.*, MOM-3 and MOM-4, E6-6 and E6-7, E6-13, *etc.*) in the range of resistances from 0.1 to 10^{13} Ohm. The samples are pressed under the pressure of $(5\div 8) \cdot 10^3$ kg cm⁻² in the form of pellets whose faces are covered with a graphite layer (of a soft pencil or Aquadag) for providing the ohmic contacts with electrodes. Electrodes of stainless steel are commonly used. Experiments with other electrodes, in particular with those of nickel, showed that contact potentials at the sample–electrode boundary do not affect substantially the results of measurements. This allows one to use a two-electrode scheme. The compensation four-electrode scheme can be necessary only in the case of objects with very small resistances which are comparative with those of the contacts at the object–electrode boundary. The activation energy of conductivity E_σ (eV) is calculated from the Arrhenius temperature dependence of the specific electroconductivity σ (Ohm⁻¹ cm⁻¹) according to the formula:

$$\sigma = \sigma_0 \exp[-E/(kT)].$$

The procedure of obtaining the TVE-curves is presented in Fig. 6, *a* and *b*. A pellet of a sample is heated stepwise *in vacuo* from 100 to 400 °C at 50° intervals (the step temperatures are designated as T_{vac}). The sample is kept to a constant value of the electroconductivity at each T_{vac} (30–60 min), and this value is recorded (the corresponding values of $\log \sigma$ in Fig. 6, *a* are marked by the figures from 1 to 6). After keeping at each T_{vac} , the reversible Arrhenius dependence of electroconductivity on the temperature of a measurement is determined in the range from T_{vac} down to 20 °C, *viz.*, after heating at $T_{\text{vac}} = 100$ °C in the range from 100 °C to 20 °C, after $T_{\text{vac}} = 150$ °C in the range from 150 °C to 20 °C, *etc.* Thus, a series of the Arrhenius straight lines is obtained, each line with its own slope (the corresponding activation energies are designated by symbols from E_1 to E_6).

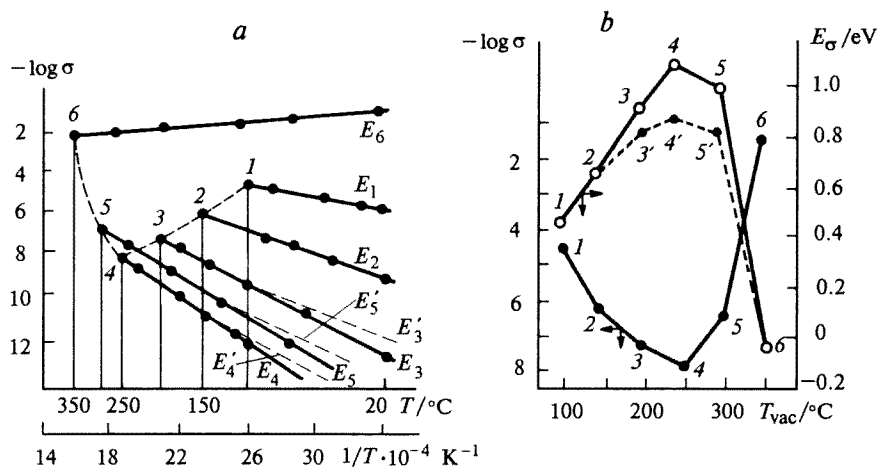


Fig. 6. Arrhenius dependences of the conductivity (a) of the NiO sample evacuated at $T_{\text{vac}} / ^\circ\text{C}$: 100 (1), 150 (2), 200 (3), 250 (4), 300 (5), 350 (6), and the TVE-curves (b) obtained for $\log \sigma$ and E_σ on the basis of this data.

As is seen in Fig. 6, *b*, one can obtain the TVE-curves of two types: for the values of $\log \sigma$ and E_σ . In the method described, the E_σ values characterize the changing energetics of successive desorption and topochemical processes rather than a zone structure of the object under study. Therefore, the TVE-curves with using E_σ are the mirror reflections of the TVE-curves with using $\log \sigma$, however, sometimes one type proves to be more informative than the other and can have another shape, *viz.*, as in the case of ferrites.

Dashed lines in Fig. 6, *b* describe the case of a "break" in the Arrhenius straight line, *i.e.*, the appearance of two different values of the activation energy of conductivity (E_σ and E_σ'), which characterize the object in the high- and low-temperature regions of measurements, respectively. As a result, the TVE-curve in the $E_\sigma - T_{\text{vac}}$ coordinates is broken for two branches concerning to different surface phases.

It is shown for the example of NiO (Fig. 7) how a characteristic band is obtained for each individual substance from a number of TVE-curves measured on samples of this substance of various origins; this band is used as the standard for the surface phase analysis. The width of the band at each temperature corresponds to a random "biographic" scattering that can amount to several orders, as is seen in Fig. 7. Curves 6 and 7 go beyond the standard band for NiO, indicating the presence of a phase that differs from NiO. Curve 6 corresponds to nickel hydroxide decomposed incompletely because of a too low calcination temperature (350°C), and curve 7 indicates the effect of anionic stabilization of the NiO phase, which is described in a corresponding section (p. 279).

The standard bands for a series of oxides are presented in Fig. 8. The procedure of the surface phase analysis consists in the obtaining of the TVE-curve for

the object under study followed by identification of the surface phases by graphic comparison of the curve with standard bands for those compounds whose presence is possible in this sample. If the data for obtaining the band typical of any substance is insufficient, then only one standard curve can be used for the phase analysis.

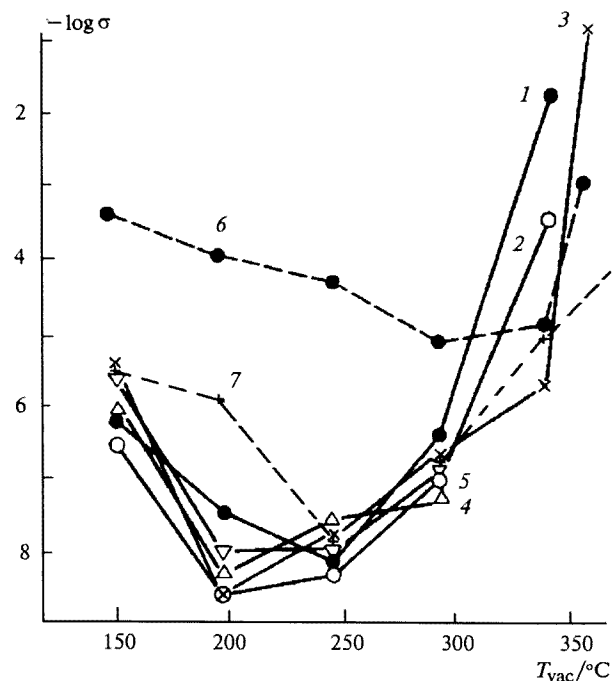


Fig. 7. TVE-curves for NiO samples obtained from nickel hydroxide at the following values of pH of precipitation and the temperature of calcination ($^\circ\text{C}$): 1, 9.3 (400); 2, 8.1 (700); 3, 9.3 (700); 4, 8.6 (430); 5, 8.9 (600); 6, 8.1 (350); 7, the NiO sample obtained by the calcination of nickel hydroxocarbonate at 700°C .

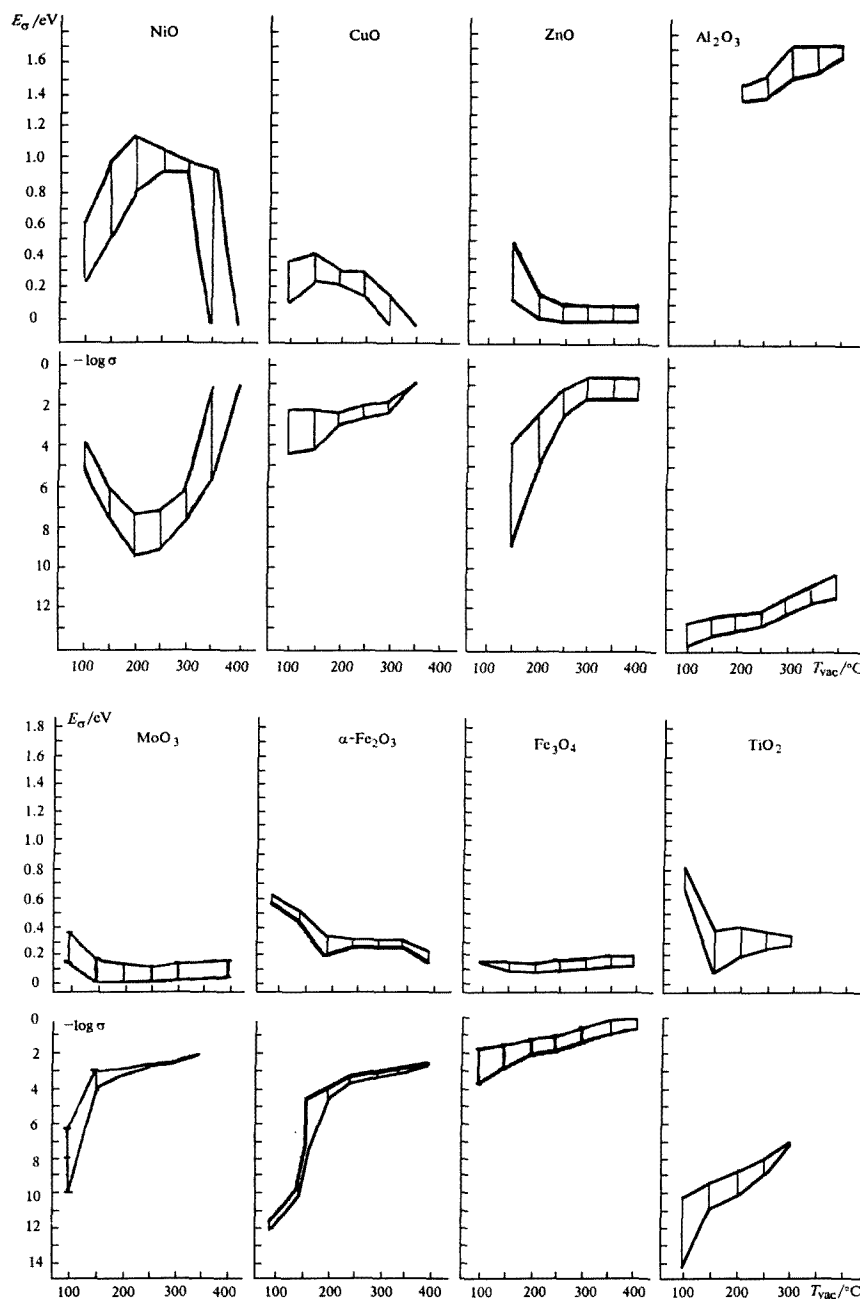


Fig. 8. Standard TVE-bands for several compounds calcined preliminarily at 400–600 °C.

The TVE-curves method is very simple and needs no thorough observing methodical conditions. A characteristic shape of the curve is retained under a change in a wide region in the pressure of pressing a pellet (100–10000 kg cm⁻²), a depth of a vacuum in a cell (from 10⁻⁶ Torr to forevacuum), dispersion of an object, thickness of a pellet, as well as under the use of various contact coverages for a pellet and various materials for electrodes. The weak effect of changes in methodical parameters on a shape of the TVE-curve can be explained on the basis of the Shklovskii theory (p. 258), according to which a great amount and variety of barriers in a barrier-disordered

object provide the relative stability of the key conductivity and smooth out a biographic scattering in the experimental values of the electroconductivity.

Use of the TVE-curves method in heterogeneous catalysis

Migration of phases in a catalyst

In order to show how the measurements of electroconductivity allow one to control the redistribution of phases in a solid, it is most convenient to begin

with considering the simplest system — a binary mechanical mixture.

Migration of the phases interacting with each other in a mechanical mixture (NiO—CuO). Figure 9 presents the results of the surface phase analysis of the mechanical mixture of nickel and copper oxides precalcined at 700 °C containing only 3 mol. % of CuO.⁶⁷ This small additive, if uniformly distributed, does not affect the electroconductivity of the system as one should expect on the basis of the percolation approach, and the mixture prepared is actually similar to NiO in its behavior (cf. curves 1 and 3). However, after calcination at 600 °C, no TVE-curve characteristic for NiO is observed but broken curve 4 which gives evidence for the formation of two new surface phases. The X-ray phase analysis of the bulk of the calcined mixture reveals coexistence of two solid solutions: CuO in the NiO lattice and NiO in the CuO lattice. Correspondingly, one should refer curve 4', which is similar to "distorted" curve 1, to the NiO-based solution and curve 4'', which is close to curve 2, to the CuO-based solution. This means that after calcination, the distribution of a small additive of CuO in a mixture becomes nonuniform. CuO in the amount of only 3 mol. % proves to be concentrated predominantly in subsurface layers and provides the formation of the subsurface infinite cluster from the CuO-based solid solution. Thus, at 600 °C, the CuO phase exhibits high migration mobility in the direction to the surface of particles as well as a capability "to spread" at surface layers.

This example allows one to consider the possibilities of the TVE-curves method with respect to one more problem. It connects with the topochemical transformations of a catalyst, the formation of the phases of an alternating composition, *viz.*, solid solutions. The appearance of two solid solutions mentioned, when

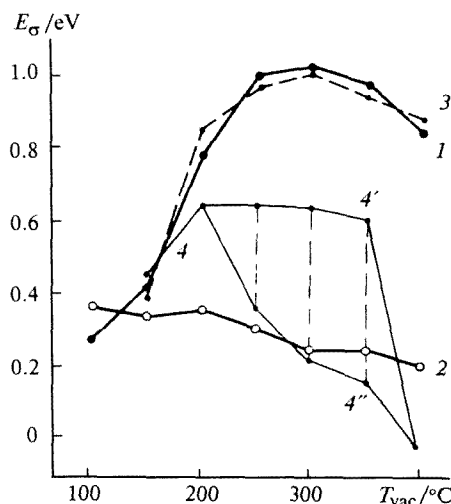


Fig. 9. The TVE-curves of the mechanical mixture of 97 mol. % NiO (700 °C) + 3 mol. % CuO (700 °C): 1, NiO (700 °C); 2, CuO (700 °C); 3, the mixture; 4—4'', the mixture after additional heating at 600 °C.

NiO+CuO mixture is calcined, occurs, on the one hand, *via* incorporation of Cu²⁺ ions into the NiO lattice and, on the other hand, *via* incorporation of Ni²⁺ ions into the lattice of the excess surface CuO phase arised due to migration of CuO to the surface of particles. The distortion of lattices of individual NiO and CuO phases due to incorporation of the extraneous ions first results in somewhat distortion of a shape of the TVE-curve, as seen in Fig. 9, and, secondly, in a shift in the position of the curve in a plot (cf. curve 1 for NiO with curves 4—4' for a solid solution of "NiO type"). Both indications (the distortion and shift of the TVE-curve) are typical of the formation of namely solid solutions rather than of stoichiometric compounds and are used for the analysis of various catalytic systems.

Initial migration of phases in precursors (nickel and copper hydroxocarbonates). When catalysts are prepared, the redistribution of phases and interaction between them begin at the initial stages of genesis of an active state in precursors and depend on the procedure of preparation. The use of the TVE-curves method *in situ* (for uncalcined samples) allows one to follow these processes. Figure 10 presents the results of the surface phase analysis of the system of nickel and copper hydroxocarbonates (precursors of oxide nickel—copper catalysts).⁶⁷ In the system with Ni : Cu = 2 : 1 atomic ratio

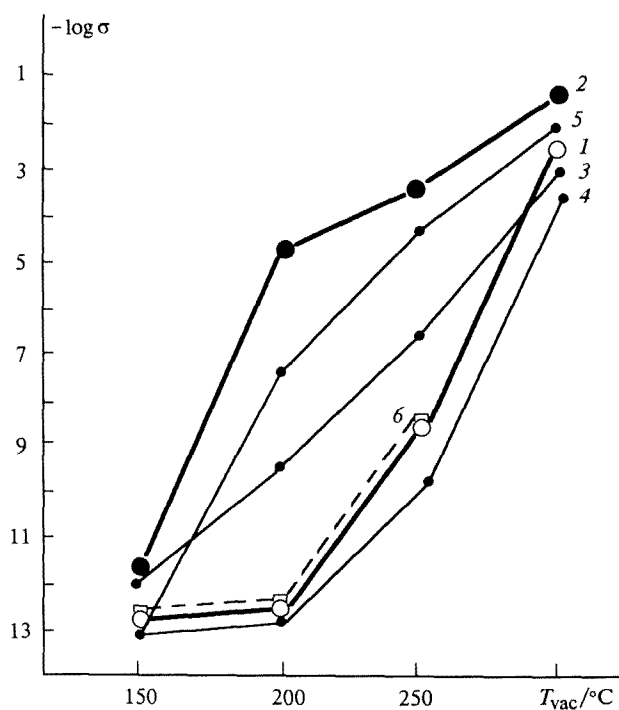


Fig. 10. TVE-curves of the uncalcined precursors of the NiO—CuO system: 1 and 2, nickel and copper hydroxocarbonates, respectively; 3 and 4, samples with the Ni : Cu = 2 : 1 ratio prepared by wet mixing and precipitation, respectively; 5, a sample with the Ni : Cu = 1 : 1 ratio prepared by coprecipitation; 6, a mechanical mixture of 67 mol. % Ni hydroxocarbonate + 33 mol. % Cu hydroxocarbonate.

prepared by coprecipitation, both at the surface and in the bulk nickel hydroxocarbonate prevails (curve 4 coincides virtually with curve 1 for pure nickel hydroxide). It follows that in coprecipitated samples as in a mechanical mixture (curve 6), the surface is not enriched by copper containing compound. Curve 5 obtained for the coprecipitated sample with a greater concentration of copper containing compound ($\text{Ni} : \text{Cu} = 1 : 1$) is close to curve 2 for pure copper hydroxocarbonate indicating somewhat enrichment of the surface by copper-containing compound, *viz.*, its possible migration. When the same system is obtained by wet (chemical) mixing, the formation of the surface solid solution of an intermediate mixed type is observed even in the sample in which a "nickel" component prevails (curve 3). This points undoubtedly to the enrichment of the surface by a "copper" component, *viz.*, its facilitated migration under the conditions of chemical mixing.

Chemical interaction in a catalyst to form solid solutions

Systems with unlimited mutual solubility of components ($\text{NiO}-\text{MgO}$). By means of XRD, IR spectroscopy, DTA, and ESR techniques, the existence of a continuous row of solid solutions in the coprecipitated $\text{NiO}-\text{MgO}$ system calcined at 700°C , which arise at the stage of hydroxides, has been established.^{58,68} These solutions are nonuniform: Ni^{2+} ions form associates (clusters).⁶⁹ The TVE-curves of two types obtained (Fig. 11) allow one, together with magnetic data, to reveal NiO clusters of two

types depending on the components ratio. The dependence of the electroconductivity on the concentration in this system is of a percolation nature (see p. 260). In the before-threshold region at a NiO concentration from 1 to 15 mol. %, only "small" clusters form (curves 2–5 are close to curve 1 obtained for MgO). In the after-threshold region, starting from ≈ 30 mol. % NiO , "large" clusters appear, which are the nuclei for the NiO crystallites (curves 6–8 in shape are classed as NiO type). It is also established that in the catalysts calcined at 700°C , NiO clusters are nonuniformly distributed between the bulk and the surface, and the calcination at 1100°C not only eliminates this nonuniformity of the system, but also results in the disappearance of large clusters. Thus, the TVE-curves method allows one "to decode" the phase composition of the object and follow its transformations in the course of the percolation process.

The catalytic activity of the system under discussion in the reactions of the N_2O decomposition⁷⁰ correlates well with a change in the surface phase composition (Fig. 12). In a series of the catalysts calcined at 700°C , the samples containing small clusters are characterized by E_a values that fall into a dashed region of average values. One can conclude that the large clusters are more active than the small ones. In the case of a mechanical mixture of Ni and Mg oxides calcined at 700°C , the low value of E_a is already observed at only 3 mol. % NiO (point 3). It is due to that NiO in a mechanical mixture exists in a free state. In a series of more uniform coprecipitated catalysts obtained at 1100°C (curve 2), the catalytic behavior of solid solutions is due to less active small clusters, and the activity of pure NiO phase decreases because of sintering (annealing of defects) which is prevented by Mg^{2+} ions in the region of solid solutions.

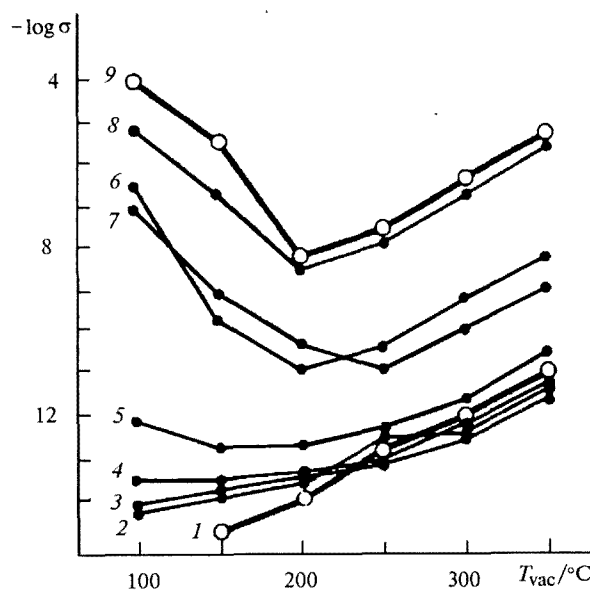


Fig. 11. Electrical characteristics (the TVE-curves) depending on the composition of $\text{NiO}-\text{MgO}$ system (700°C): 1, MgO ; 2, 1 mol. % NiO ; 3, 3 mol. % NiO ; 4, 10 mol. % NiO ; 5, 15 mol. % NiO ; 6, 29 mol. % NiO ; 7, 60 mol. % NiO ; 8, 91 mol. % NiO ; 9, NiO .

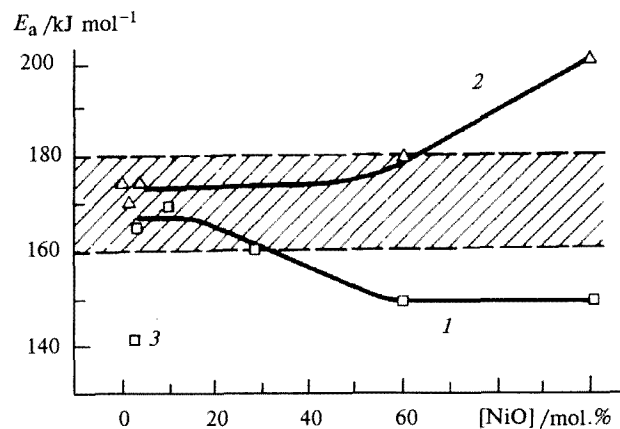


Fig. 12. Energy of activation of the N_2O decomposition depending on the composition of the $\text{NiO}-\text{MgO}$ catalysts calcined preliminarily at 700°C (1) and 1100°C (2); 3, the mechanical mixture of 3 mol. % $\text{NiO}+97$ mol. % MgO (700°C). The dashed region is the region of the average E_a values.

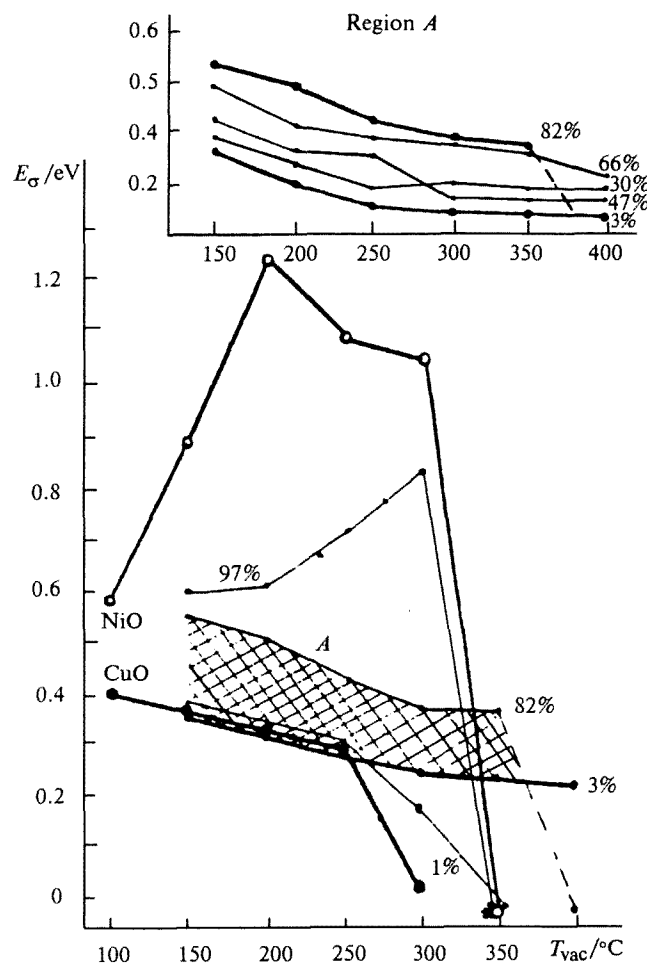


Fig. 13. Electrical characteristics (the TVE-curves) of the NiO–CuO system (700 °C). Numbers near the curves represent the NiO content (mol. %) in this sample.

Systems with limited mutual solubility of components (NiO–CuO). Nickel and copper oxides interact readily. As was above mentioned, the formation of solid solutions is observed already in the NiO+CuO mechanical mixture when they are heated (p. 268). According to the XRD data, in the bulk of the NiO–CuO system prepared by coprecipitation with an aqueous solution of ammonia from aqueous solutions of nitrates, the limited solid solutions of substitution form (below 5 mol. % NiO in CuO and below 25 mol. % CuO in NiO). The surface phase analysis (Fig. 13) reveals substantial differences between the surface and bulk compositions.^{71–73} In a series of the samples calcined at 700 °C, in a wide range of the NiO content from 3 to 82 mol. % (see region A), virtually the same TVE-curves of a CuO-type are retained. However, these curves differ from the TVE-curve for the individual CuO phase by the absence of a sharp drop in the E_σ value to ≈ 0 in the region of high T_{vac} . Such a drop in the E_σ values and the corresponding growth in the electroconductivity is commonly observed

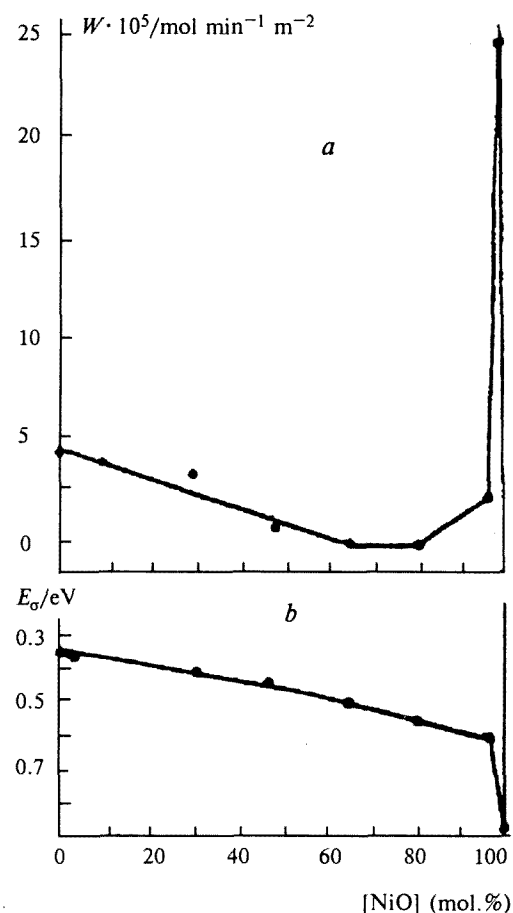


Fig. 14. Dependence of the catalytic activity in N_2O decomposition (a) and the activation energy of conductivity E_σ (b) of the NiO–CuO (700 °C) system on its composition.

at T_{vac} 300–350 °C and gives evidence for the reduction of CuO to Cu. The result obtained means that the surface of the catalysts with the compositions mentioned is covered with the solid solution of NiO in CuO, in which CuO is stabilized against reduction. This confirmed the conclusion on the high migration mobility of the CuO phase. On the other hand, when the NiO phase prevails (97 mol. %), the TVE-curve is close to that of a NiO type and consequently reveals the second solid solution at the surface, the NiO-based solution (CuO in NiO).

The catalytic activity of this system also correlates well with the surface composition estimated.⁷¹ In the region of the CuO-based solid solution (3–82 mol. % NiO), the activity in the decomposition of N_2O lowers smoothly (Fig. 14, a) as the hole conductivity becomes weaker with a rise in the nickel content (see Fig. 14, b). A decrease in the activity is apparently due to the progressive impeding of the donor rate-determining step (desorption of O_2). In the region of the NiO-based solid

solution (97 mol. % NiO), the activity drops as compared to the individual NiO phase (see Fig. 14, *a*); respectively, a jump-like increase in the hole conductivity is observed when CuO is added to NiO (see Fig. 14, *b*). This drop in activity can be explained by impeding the acceptor stage (adsorption of N_2O) which becomes a rate determining step.

It should be emphasized that it is very difficult to obtain by other techniques the information about the formation of the surface solid solutions given by the TVE-curves method (as is described in this section and further). Thus, the XPS technique points to the quantitative ratio of ions at the surface, *viz.*, Ni^{2+} and Cu^{2+} , but does not allow one to conclude definitely whether the corresponding Ni and Cu oxides are present separately or form a solid solution.

Chemical interaction to form a new compound

Systems without mutual solubility of components ($NiO-TiO_2$). When the $NiO-TiO_2$ system is prepared by coprecipitation, one expects to obtain a uniform distribution of NiO in the matrix of the inert support, because TiO_2 in a mechanical mixture with NiO forms no chemical compounds at temperatures below 1000 °C and, unlike MgO and CuO , does not form any solid solutions.⁷⁴⁻⁷⁶

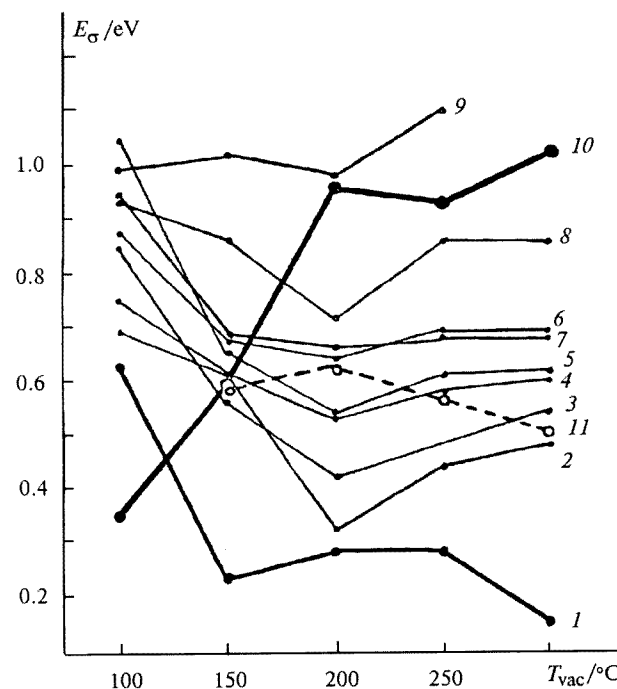


Fig. 15. Electrical characteristics (the TVE-curves) depending on the composition of the $NiO-TiO_2$ system (430 °C): 1, TiO_2 ; 2, 1 mol. % NiO; 3, 5 mol. % NiO; 4, 12 mol. % NiO; 5, 23 mol. % NiO; 6, 35 mol. % NiO; 7, 60 mol. % NiO; 8, 80 mol. % NiO; 9, 96 mol. % NiO; 10, NiO; 11, an equimolar mechanical mixture of NiO (430 °C) + TiO_2 (430 °C).

However, the surface phase analysis of the samples of this system calcined at 430 °C (Fig. 15) revealed a new phase that is formed already at this temperature and differs by the TVE-curves from both NiO and TiO_2 . The presence of this phase determines the nature of the conductivity of the system in a very wide range of compositions (curves 2–8). As only 1 mol. % of the NiO additive is sufficient for arising of a new phase, it is obvious that this phase covers the surface of the catalyst with a thin layer.⁵⁷ It is identified as nickel titanate ($NiTiO_3$), because a rise in the calcination temperature to 600 °C did not result in a change in the surface composition, but the lines of $NiTiO_3$ bulk phase appeared on diffractograms which were absent after calcination at 430 °C. Thus, when a new phase appears in the region of intergranular contacts at the surface layer, the TVE-curves method proves substantially more sensitive than XRD and reveals the initial stage of the formation of "low-temperature" $NiTiO_3$ already at 430 °C.

The approach on the basis of the TVE-curves method described allows one to avoid an error when analyzing a system with a "electroconductivity—composition" diagram. On the basis of a drop in the electroconductivity, when small additives of the second component at both edges of a scale of compositions are introduced (this corresponds formally to the Verwey rule), one could make a conclusion on the formation of mutual solid solutions (see p. 262). It has been made just such a suggestion by the authors of work,⁷⁷ who found a drop in electroconductivity in $NiO-TiO_2$ system with a rise in NiO content from 0.41 to 1.61 mol. % and ascribed this effect to the formation of a solid solution. The TVE-curves method allowed one to establish that the real reason for jumps in the electroconductivity is the formation of surface nickel titanate. No solid solutions form in this system (the parameter of oxide lattice in mixed samples remains constant); consequently, the correspondance of changes in the electroconductivity to the Verwey rule is only an accidental.

The registration of changes in a work function which is due to the additive contribution of potentials of all surface phases, serves as the addition to the results of the surface phase analysis.^{78,79} In the range of compositions of 23–35 mol. % NiO, the surface is completely covered with nickel titanate; in the range of 0–23 mol. % NiO, the TiO_2 and $NiTiO_3$ phases coexist and in the range of 35–100 mol. % NiO, the $NiTiO_3$ and NiO phases do so. The results obtained can explain the catalytic behavior of the system in the decomposition of N_2O . The activity decreases with a decrease in the NiO concentration in the range from 100 to 35 mol. % of NiO and then remains at the very low level.^{57,58} This is in line with the fact established that the NiO active phase is completely screened by the surface layer of inactive $NiTiO_3$ at the NiO content which is not higher than 35 mol. %.

Systems containing solid solutions with a compound formed ($NiO-MoO_3$). The results of the surface phase analysis of a series of the $NiO-MoO_3$ catalysts prepared

by wet interaction of oxides^{80,81} (Fig. 16) show that the samples studied are divided for three groups by a type of the TVE-curves, *viz.*, for the surface composition. 1) MoO_3 type is described by curves 1 and 2, which represent the range of compositions of 9–33 mol. % NiO and virtually fall into a standard band 7 for MoO_3 phase. 2) NiO type is described by curve 4, which depicts the composition with 91 mol. % of NiO and is close in a shape to curve 5 for NiO ; however, the maximum in the region of T_{vac} 200–300 °C typical of NiO is substantially smoothed down. 3) Nickel molybdate type is described by curve 3 (the sample with 64 mol. % NiO), which only slightly differs from curve 6 for NiMoO_4 phase.

It follows that at the NiO content not higher than 33 mol. %, the MoO_3 -based solid solution, whose formation is confirmed by X-ray phase analysis, is present at the surface. A proximity of curve 3 to curve 6, which describes standard nickel molybdate NiMoO_4 , means that with a rise in the NiO content (to 64 mol. %), a new phase forms which should be identified as a nickel molybdate. In the region of high NiO concentration (91 mol. %), the surface NiO -based solid solution forms. It can be only the NiMoO_4 – NiO solid solution rather than MoO_3 – NiO , because in this system (similarly to the NiO – TiO_2 system), dissolution of MoO_3 in NiO is ruled out. According to the principle of controlled valency, doping cations of higher valence (Mo^{6+}), which substitute for cations in the lattice of p-semiconductor oxide (NiO), should increase its electrical resistance and the activation energy of conductivity, but in our experiment, the E_{σ} value drops when small additions of MoO_3 are introduced.

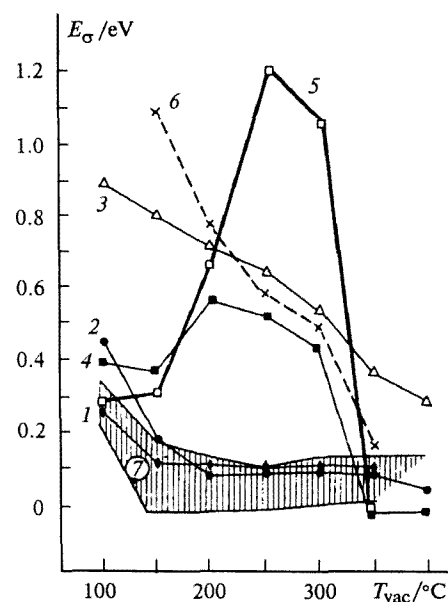


Fig. 16. TVE-curves for the samples of the NiO – MoO_3 system (550 °C): 1, 9 mol. % NiO ; 2, 33 mol. % NiO ; 3, 64 mol. % NiO ; 4, 91 mol. % NiO ; 5, NiO ; 6, NiMoO_4 ; 7, the standard band of MoO_3 .

The results of the surface phase analysis obtained allow one to explain why the catalytic activity of NiO in the reaction of N_2O decomposition drops when introducing a small amount (9 mol. %) of MoO_3 .⁸⁰ It is obvious that the formation of the surface solid solution of nickel molybdate in NiO results in distortion of the NiO lattice and consequently deactivation of the catalyst.

Interaction of an active phase with a support (percolation aspect)

Effect of strong metal–support interaction (Ni – TiO_2). A number of works carried out with the use of modern techniques are devoted to the effect of strong metal–support interaction (SMSI); however, in a number of real systems the nature of SMSI remains unclear.⁵⁰ The TVE-curves method gives new information on the processes connected with this effect, for example, for partial reduction of the NiO – TiO_2 system.⁸² It follows from Fig. 17 that reduction at 500 °C results in the transformation of the semiconductor NiO – TiO_2 system (see Fig. 15) to a pseudometallic system with a very low activation energy of conductivity (curve 1). The nickel metal formed is not observed: the nickel-containing sample (curve 1)

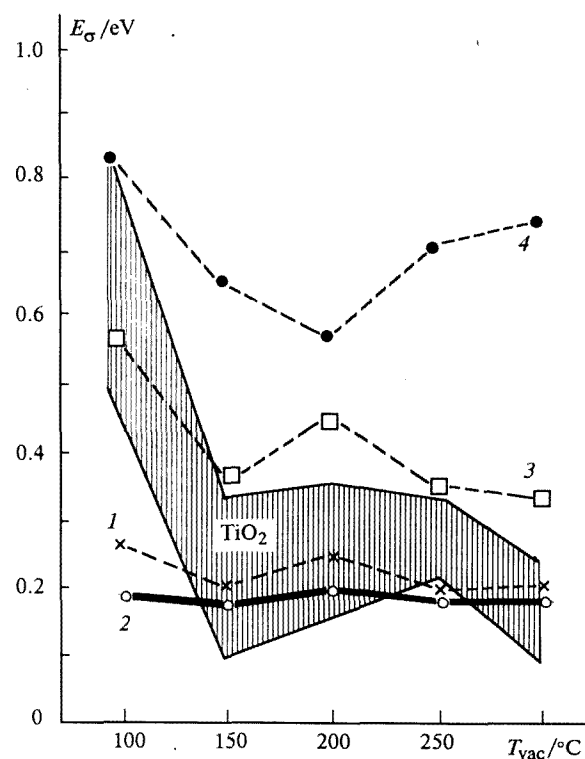


Fig. 17. Influence of reduction on the electrical characteristics of the NiO – TiO_2 system (430 °C), the SMSI effect: 1, the sample with 23 mol. % of NiO reduced at 500 °C; 2, TiO_2 support reduced at 500 °C; 3, the sample with 23 mol. % of NiO reduced at 350 °C; 4, NiTiO_3 (430 °C).

does not exhibit better conductivity as compared to the reduced support (curve 2). The surface phase with good conductivity found in these samples is the deficient phase of lower TiO_x oxide (with oxygen vacancies in a lattice), whose presence in the bulk of the reduced system is confirmed by the XRD and magnetic susceptibility data.

Another picture is observed for the catalysts prepared by milder reduction of the $\text{NiO}-\text{TiO}_2$ system at 350 °C. The reduced system remains semiconductor, but the TVE-curves method reveals the phase of TiO_2 type instead of titanate (see Fig. 17, curve 3, which is similar in a shape to the dashed band for TiO_2). This means that the very dilute solid solution of NiO in TiO_2 (of the $\text{Ni}_8\text{Ti}_{1-\delta}\text{O}_2$ composition), whose formation stabilizes the lattice of titanium oxide, is present at the surface of this sample rather than the titanate which is characterized by a minimum on the curve at T_{vac} 200 °C (curve 4). It is noteworthy that in this case the nickel metal also does not manifest itself. According to the adsorption, X-ray, and magnetic data, this is due to the fact that contacts between nickel crystallites at the surface become difficult because of a partial screening, or "decoration," of the metallic surface owing to the accumulation of the material of the support on the particles of the metal. This is one of the mechanisms of the SMSI effect.⁵⁰ Clearly this prevents the formation of the infinite nickel cluster and development of the nickel phase (this is an example of hampered percolation).

Information about the formation of the layer of the TiO_2 -based solid solution at the surface under mild reduction of the $\text{NiO}-\text{TiO}_2$ system and its role in the SIMS effect is unique. It is difficult to obtain this information with any other technique.

Effect of strong oxide–oxide interaction ($\text{MnO}_x-\text{SiO}_2$). According to the literature data,⁸³ heating the $\text{MnO}_2-\text{SiO}_2$ mixtures to 350–400 °C causes no chemical interaction. Our studies of $\text{MnO}_2-\text{SiO}_2$ system prepared by impregnation and calcined at 500 °C confirm this result.⁸⁴ The data on electroconductivity provide evidence for percolation behavior of this system typical of a binary mechanical mixture: at the content of the MnO_2 semiconductor oxide below 12 mol. %, all TVE-curves remain in the region of dielectric SiO_2 , and the addition of 19 mol. % MnO_2 causes a jump-like rise in the conductivity and the corresponding lowering in E_σ . The TVE-curves for all samples containing ≥ 19 mol. % of MnO_2 are located in the region of standard band of MnO_2 , which is due to percolation, *i.e.*, a flow of electric current through the chain of continuous contacts between MnO_2 particles. Figure 18 presents this data as the dependence of the activation energy of conductivity on the volume concentration of components. The threshold of a percolation jump observed on curve 1 (19 mol. % MnO_2) corresponds to ~ 15 vol. % MnO_2 which is close to the theoretical value calculated on the basis of percolation models for a uniform mechanical mixture (15–25 vol. % depending on parameters of calculation).³⁰ The absence

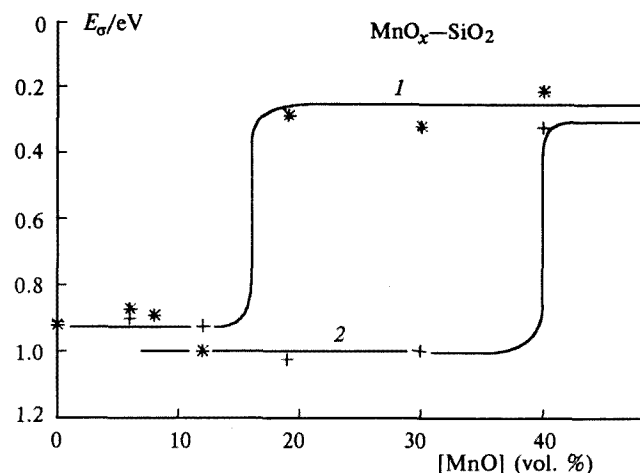


Fig. 18. Concentration dependences of the activation energy of conductivity for the $\text{MnO}_x-\text{SiO}_2$ system: the starting $\text{MnO}_2-\text{SiO}_2$ system (500 °C) (1) and $\text{Mn}_3\text{O}_4-\text{SiO}_2$ system obtained by the redox treatment at 500 °C (2).

of the interaction in $\text{MnO}_2-\text{SiO}_2$ system at 500 °C is also confirmed by the additivity of the values of the specific surface area of MnO_2 and SiO_2 found at different ratios of these components.⁸⁴

However, more detailed studies showed that in this system, under definite conditions, the substantial interactions of a special nature can occur. The surface phase analysis revealed that successive redox treatment of the $\text{MnO}_2-\text{SiO}_2$ system at 500 °C resulted in the transformation of phase-structural state of the surface. In this series of the samples (curve 2), the percolation jump is observed at the significantly higher content of manganese oxide (40 vol. %), which transforms from MnO_2 to Mn_3O_4 after treatment. An increase in the percolation threshold is not connected with a change in the dispersion of manganese oxide. Really, according XPS data, the size of crystallites of Mn_3O_4 (60–100 Å) is lesser than that of MnO_2 (120–220 Å). The appearance of more dispersed Mn_3O_4 crystallites would facilitate the formation of percolation cluster and, hence, to lower the percolation threshold rather than to heighten it. It is important for the explanation of hampered percolation that after redox treatment, a fraction of the surface of supported Mn_3O_4 becomes inaccessible for chemisorption, *i.e.*, proves to be screened by a support. The conclusion can be drawn that the treatment at 500 °C mentioned transforms the system of not interacting $\text{MnO}_2-\text{SiO}_2$ oxides into the $\text{Mn}_3\text{O}_4-\text{SiO}_2$ system with the strong interaction of oxide–oxide type whose mechanism is not of chemical nature.^{54,55} By analogy with one of the supposed mechanisms of the effect of the strong interaction oxide–oxide, one can suggest that in this case, an encapsulation process occurs,⁵⁰ *viz.*, a partial immersion of the Mn_3O_4 crystals into the bulk of a support. The catalytic behavior of the $\text{MnO}_x-\text{SiO}_2$ sys-

tem, which was evaluated by its activity in the reaction of complete oxidation of CH_4 catalyzed by manganese oxides, is in line with changes in the phase-structural state of the surface described: the CH_4 conversion decreases sharply after redox treatment of the catalyst samples.

Similar comparison of the percolation thresholds for the oxide—aluminocalcium cement systems showed that the strength of the bond of oxides with a support decreases in the sequence $\text{NiO} > \text{CuO} > \text{ZnO}$.⁵⁹ In the ZnO —cement system, the introduction of excess Al_2O_3 still more weakened the bond of ZnO with the support and increased the concentration of free ZnO at the surface, respectively. This allowed one to optimize the catalytic properties of ZnO —cement system in the industrial processes of hydrotreatment of natural and industrial gases.

The examples presented and the data for the NiO — MgO system discussed above show the advantages of percolation approach for the elucidating of the nature of interaction in solid semiconductor systems. The use of the TVE-curves method in these measurements extends the possibilities of the percolation analysis because allows one not only to fix the arising of a new conducting phase but also identify it qualitatively.⁸⁵

Distribution of phases in multicomponent systems

Coexistence of several solid solutions (NiO — CuO —cement). In the past few years, catalysts based on aluminocalcium cements have been widely used in various processes, because they combine high activity with enhanced thermal stability, mechanical strength, and stability to coke formation and they can be obtained by the topochemical reaction of components using an ecologically pure technology without waste waters. Among the catalysts of a new generation, the NiO — CuO —talume system is the most thoroughly studied with the TVE-curves method (talume is a chemical mixture of calcium monoaluminate $\text{CaO} \cdot \text{Al}_2\text{O}_3$, CA, with dialuminate $\text{CaO} \cdot 2\text{Al}_2\text{O}_3$, CA₂). Cement-containing systems are obtained by chemical mixing of Ni and Cu hydroxocarbonates with CA and CA₂ in the presence of aqua ammonia.^{86,87} With the use of XRD, DTA, and IR spectroscopy techniques it was found that in this case solid solutions of Ni and Cu hydroxoaluminates form, whose presence at the surface can be established by the TVE-curves method. The surface phase analysis of the oxide NiO — CuO —talume system formed during calcination of the precursors mentioned at 400 °C (Fig. 19) reveals several solid solutions. First, these are the solid

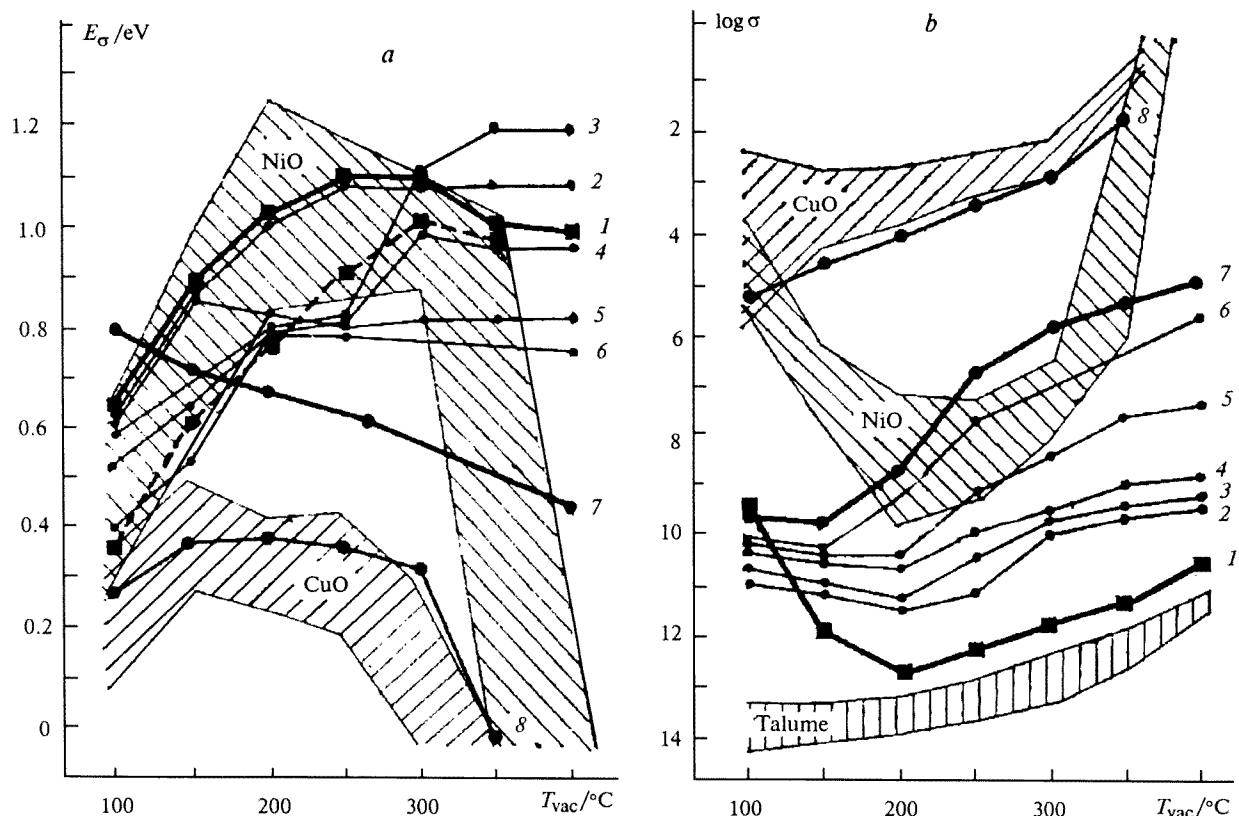


Fig. 19. TVE-curves using E_σ (a) and $\log \sigma$ (b) values for the NiO — CuO —cement samples of a various composition (wt.-%): 1, 35 % NiO —0 % CuO ; 2, 30 % NiO —5 % CuO ; 3, 25 % NiO —10 % CuO ; 4, 20 % NiO —15 % CuO ; 5, 15 % NiO —20 % CuO ; 6, 5 % NiO —30 % CuO ; 7, 0 % NiO —35 % CuO ; 8, 100 % CuO .

solutions on the basis of NiO and CuO: the NiO type, the solution of Al_2O_3 in NiO (curve 1); the CuO type, the solution of Al_2O_3 in CuO (curves 5–7); the mixed type, the solution of Al_2O_3 in the NiO–CuO solid solutions (curves 2–4). After sintering of the surface solid solutions mentioned, two solid solutions on the basis of aluminum oxide can also be developed: NiO in Al_2O_3 (see Fig. 19, a, curves 2 and 3 in the region T_{vac} 300–350 °C) and CuO in Al_2O_3 (see p. 277). The first three solid solutions are responsible for the catalytic activity of the system in the reaction of O_2 hydrogenation (Fig. 20), which is used for purification of industrial gases. The CuO-based solid solutions differ by somewhat higher level of activity (band A) than the NiO-based solid solutions (band B).⁸⁸ The relative constancy in the activity level with a change in a composition of a catalyst within each activity band as well as the stability of the active surface toward moderate heating (650 °C) give evidence for the formation in the cement-containing catalysts of a specific methastable structure which provides their high activity. Destruction of this specific structure, which occurs, for example, under insufficiently fast cooling of the catalyst after the reaction in the presence of the O_2 admixture, results in significant deactivation (see Fig. 20, points along the straight line C). The XPS data confirm this conclusion. In the active catalyst, the state of Ni^{2+} in surface solid solutions is stabilized and nickel cations can be reduced to Ni^0 at 300 °C only for 60 %, whereas after the thermal deactivation mentioned, reduction occurs completely already at 250 °C.⁸⁹

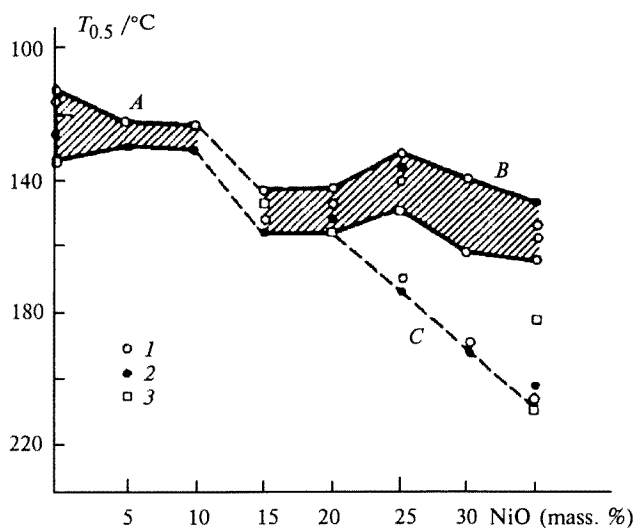


Fig. 20. Dependence of the temperature of 50 % conversion ($T_{0.5}$) of oxygen in the reaction of its hydrogenation on the composition of the NiO–CuO–cement catalysts: 1, starting samples (calcined at 400 °C); 2, samples after moderate overheating (650 °C); 3, catalysts prepared repeatedly. A, the region of enhanced activity (CuO-based solid solutions); B, the region of reduced activity (NiO-based solid solutions); C, the region of deactivation.

Data on the formation of surface solid solutions were also obtained for the Co_3O_4 –CuO–aluminocalcium cement system, and the presence of cement in this case also facilitates the formation of solid solutions between components.⁹⁰

Anchored surface phases (supported chlorides). Various chlorinated hydrocarbons which are widely used as industrial chemicals and solvents, can be obtained by the processes of oxidative chlorination at 350–400 °C, which are efficiently catalyzed by impregnated systems containing CuCl_2 (or $\text{CuCl}_2\text{–KCl}$) on Al_2O_3 (or SiO_2) with the content of a salt component of $12 \cdot 10^{-4}$ g-ion g^{-1} of a catalyst. It is shown with the DTA method that the salt component interacts chemically with the support upon fusion and forms various compounds which participate in catalysis. The surface phase analysis of these catalysts is an example of the use of the TVE-curves method in an *in situ* version (for the samples which underwent no preliminary heating). These catalysts are hereinafter referred as $\text{KCuAl}(\alpha, \gamma)\text{–Si}$, where $\text{K} = \text{KCl}$, $\text{Cu} = \text{CuCl}_2$, $\text{Al}(\alpha, \gamma) = \alpha$ - and γ - Al_2O_3 , $\text{Si} = \text{SiO}_2$.⁹¹

Figure 21 presents the behavior of the starting salts, oxides, and binary systems under heating in a vacuum. The enhanced values of electroconductivity and low

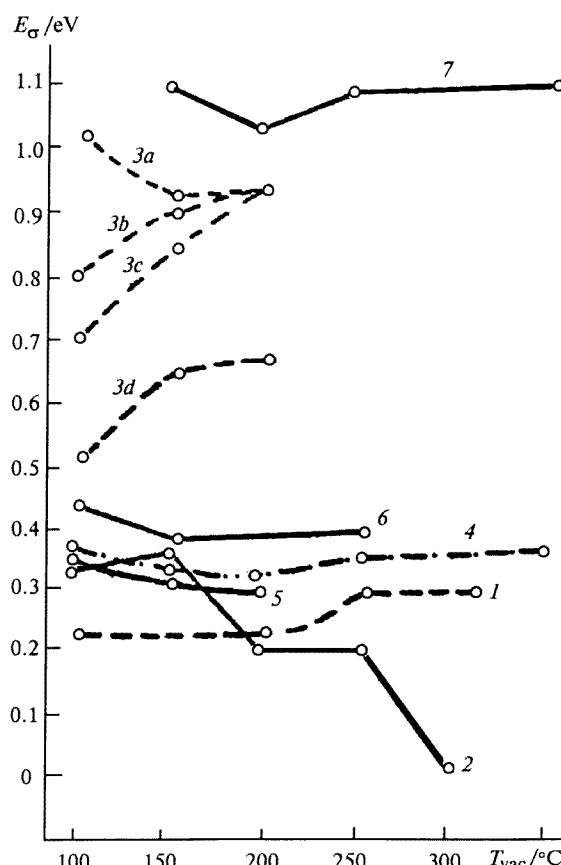


Fig. 21. TVE-curves for binary chloride systems and supports: 1, K ; 2, Cu ; 3, KCu ; a–d, for pellets prepared repeatedly; 4, $\text{Al}(\alpha)$; 5, $\text{Al}(\gamma)$; 6, $\text{CuAl}(\alpha)$; 7, $\text{KAl}(\alpha)$.

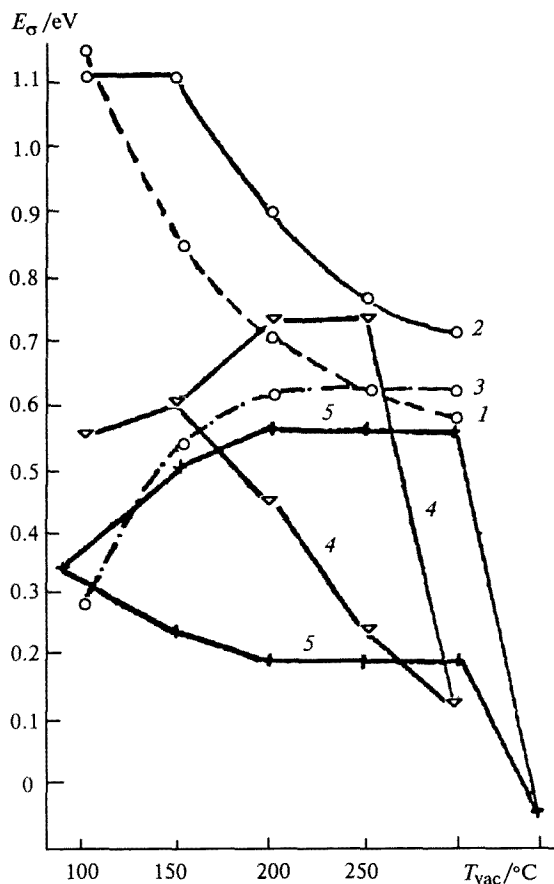


Fig. 22. TVE-curves for ternary chloride systems: 1, $KCuAl(\alpha)$; 2, $(Cu+K)Al(\alpha)$; 3, $(K+Cu)Al(\alpha)$; 4, $KCuAl(\gamma)$; 5, $KCuSi$.

values of E_σ for KCl , $CuCl_2$, and Al_2O_3 (curves 1, 2, 4, 5) are caused by the effect of superionic conductivity due to impurities (in particular, β - Al_2O_3 and hydrochlorides). Deposition of $CuCl_2$ on Al_2O_3 has nearly no effect on the electrical properties of oxides (cf. curves 4 and 6), whereas after introduction of KCl , potassium aluminates form and the state of superionic conductivity is distorted. As a result, the electroconductivity lowers by a few orders and E_σ strongly increases (cf. curves 4 and 7). The excessive KCl is distributed at the surface as isolated islands and does not form a general percolation cluster as can be judged from the distance between curves 7 and 1. The electroconductivity of supported binary KCu system is very sensitive to a biography (curves 3a–3d) and becomes unstable after fusion (above 200 °C).

In ternary systems the picture is different (Fig. 22). The $KCuAl(\alpha)$ system obtained by combined supporting of KCl and $CuCl_2$ on α - Al_2O_3 (curve 1) does not resemble in the character of the TVE-curves any one of the binary systems considered, and under successive deposition, the results depend on the order of introduction of components. If $CuCl_2$ is first supported, then the $(Cu+K)Al(\alpha)$ system below T_{vac} 150 °C is close to $KAl(\alpha)$ binary system (see Fig. 21, curve 7) by the TVE-curve

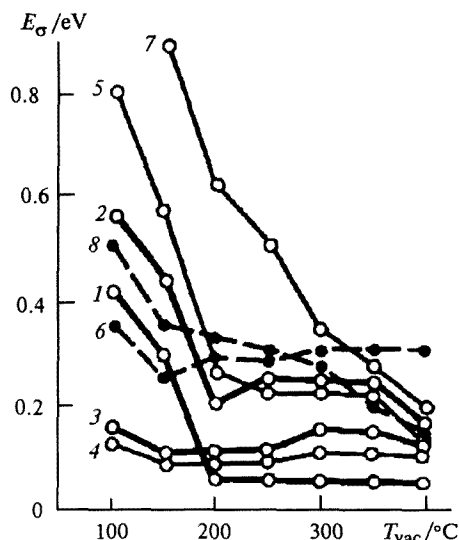


Fig. 23. TVE-curves for the oxides and binary combinations in the $ZnO-Fe_2O_3-Al_2O_3$ system: 1, ZnO ; 2, α - Fe_2O_3 ; 3, Fe_3O_4 ; 4, $ZnO-Fe_2O_3$ prior to performance; 5, $Fe_2O_3-Al_2O_3$ prior to performance; 6, $Fe_2O_3-Al_2O_3$ after reaction; 7, $ZnO-Fe_2O_3-Al_2O_3$ prior to performance; 8, $ZnO-Fe_2O_3-Al_2O_3$ after reaction.

(curve 2), and under further heating in a vacuum, its behavior is the same as that of $KCuAl(\alpha)$ (see Fig. 22, curve 1). If KCl is first supported and $(K+Cu)Al(\alpha)$ is obtained, then the TVE-curve (curve 3) reproduces the behavior of methastable states of the KCu system (see Fig. 21, curve 3d). In spite of these differences, it is seen that after heating at T_{vac} 300 °C, curves 2 and 3 (see Fig. 22) nearly coincide with curve 1. Apparently, at the surface of the heated samples, the same phases form as in the $KCuAl(\alpha)$ system. On the basis of the XRD and DTA data, one can conclude that the active catalytic surface is formed by the complex salts of $KCuCl_3$ and K_2CuCl_4 compositions which are anchored on the support. When chlorides are supported on SiO_2 , a similar picture is observed (see the upper branch of curve 5 below T_{vac} 300 °C), but in this case, one more phase is developed, possibly, the excessive $CuCl_2$ (see Fig. 21, the lower branch of curve 5 which is similar to curve 2). The heating to T_{vac} 350 °C, apparently, results in the destruction of these active salt complexes anchored on the support. When γ - Al_2O_3 is used as a support, the active complexes are anchored with a lesser strength and destructed already at T_{vac} 300 °C (curve 4).

Identification of the surface active phase

Ferrites on a support. The zinc and magnesium ferrites ($ZnFe_2O_4$ and $MgFe_2O_4$) exhibit high activity in the process of oxidative dehydrogenation of butenes to divinyl

at 500 °C and are the most active upon deposition on Al_2O_3 (by coprecipitation from oxalates). In the $\text{ZnO}-\text{Fe}_2\text{O}_3-\text{Al}_2\text{O}_3$ system calcined at 250 °C, the formation of several phases is possible. The TVE-curves method helps to reveal the surface phase that is responsible for catalytic activity of supported ferrites. With this purpose, a comparison of the activity with the surface composition for all components of this system and all binary compositions, which can form in it, has been carried out.⁹² Comparison of the curves in Fig. 23 shows that $\text{ZnO}-\text{Fe}_2\text{O}_3-\text{Al}_2\text{O}_3$ system (500 °C) before performance is the closest in its surface composition (curve 7) to the $\text{Fe}_2\text{O}_3-\text{Al}_2\text{O}_3$ binary combination (curve 5), however, the TVE-curve for the ternary system is shifted to the region of higher resistances and the values of the activation energy of conductivity. This shift can be explained by the presence of zinc aluminate ZnAl_2O_4 dielectric phase.

Comparison of the samples after treatment with a reaction mixture shows that the $\text{ZnO}-\text{Fe}_2\text{O}_3-\text{Al}_2\text{O}_3$ system in active state (curve 8) is also very close in a surface composition to the $\text{Fe}_2\text{O}_3-\text{Al}_2\text{O}_3$ binary combination (curve 6), which differs in a type of the TVE-curve and activity from its components, Fe_2O_3 (or Fe_3O_4) and Al_2O_3 . Hence, the surface phase should be iron aluminate FeAl_2O_4 , the product of the interaction of the components of this binary combination. But all aluminares are dielectrics, therefore, the enhanced conductivity of the supposed FeAl_2O_4 can be explained by the presence of the Fe_3O_4 ferrite phase that forms a solid solution with FeAl_2O_4 . Thus, it is most probable, that at the surface of the $\text{ZnO}-\text{Fe}_2\text{O}_3-\text{Al}_2\text{O}_3$ active system,

the solid solution of $\text{FeAl}_2\text{O}_4-\text{Fe}_3\text{O}_4$ ferrite structure forms which can also include zinc ferrite ZnFe_2O_4 identified by the X-ray phase analysis.

Catalysts for hydrotreatment processes ($\text{Co}_9\text{S}_8-\text{MoS}_2$). The results of the surface phase analysis of the Co-Mo-S sulfide system (Fig. 24) showed⁹³ that the components of this system in their electrical behavior are concerned to different classes of conductors: molybdenum sulfide MoS_2 (curve 1) is a typical semiconductor with the activation energy of conductivity $E_\sigma \sim 0.2$ eV, whereas cobalt sulfide Co_9S_8 (curve 2) exhibits pseudometal properties with enhanced electroconductivity that in fact does not alter with a temperature ($E_\sigma \approx 0$). In the $\text{Co}_9\text{S}_8-\text{MoS}_2$ system, independently of the preparation procedure, *viz.*, coprecipitation (curve 3) or impregnation (curve 4), both TVE-curves belong to a MoS_2 type. In fact, they are close to the TVE-curve for molybdenum sulfide in a slope and nearly straight line form but are shifted from it in the values of electroconductivity by 1–3 orders. Consequently, the main fraction of the surface of the catalysts prepared is the phase on the basis of MoS_2 . The enhanced electroconductivity, in accordance with the magnetic data, is due to the presence of Co^{2+} ions intercalated into the interlayer space of layered structure of molybdenum sulfide, *i.e.*, to the formation of the "solid solution of incorporation" of Co_9S_8 in MoS_2 . Comparison with the TVE-characteristics for several mechanical $\text{Co}_9\text{S}_8+\text{MoS}_2$ mixtures allowed one to conclude on the enrichment of the surface of coprecipitated and impregnated systems by the phase of the solid solution formed. This conclusion is in line with the XPS data.

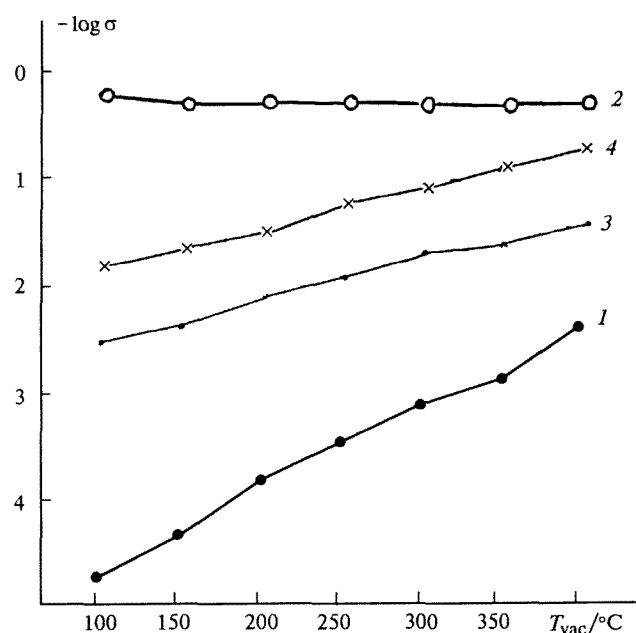


Fig. 24. TVE-curves for the Co-Mo-S system with the $\text{Co}/(\text{Co}+\text{Mo}) = 0.4$ ratio: 1, MoS_2 ; 2, Co_9S_8 ; 3, the coprecipitated catalyst; 4, the impregnated catalyst.

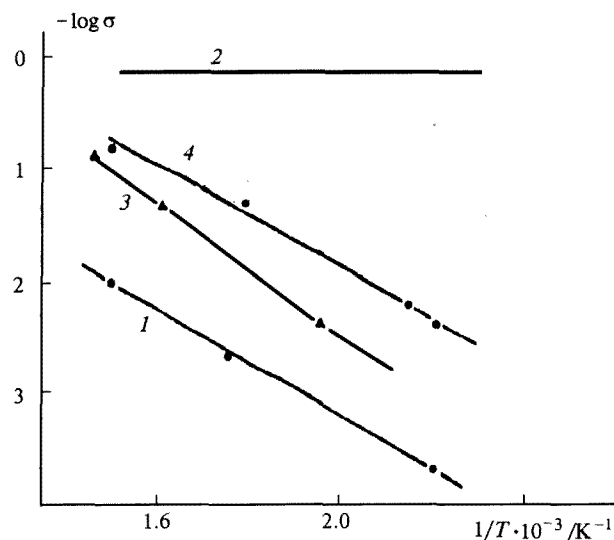


Fig. 25. Temperature dependences of electroconductivity (in the Arrhenius coordinates) for the Co-Mo-S system with $\text{Co}/(\text{Co}+\text{Mo}) = 0.3$ ratio:⁹⁴ 1, MoS_2 ; 2, Co_9S_8 ; 3, precipitated catalyst; 4, impregnated catalyst.

Thus, the analysis performed not only confirmed the numerous literature data on the role of so-called Co—Mo—S phase as the active phase of sulfide catalysts of hydrotreatment but also made it possible to conclude about the nature of this active phase as the Co_9S_8 — MoS_2 solid solution.

Interesting conclusions can be drawn from a comparison of our data with the results on measurements of the same system carried out with a direct current but without using the TVE-procedure.⁹⁴ The authors presented their results in the Arrhenius coordinates (Fig. 25). The plot obtained nearly exactly coincides with our plot in Fig. 24 as its mirror reflection because of the opposite direction of a temperature axis. This coincidence is due to that for both components of the Co_9S_8 — MoS_2 system, the TVE-curves are nearly straight lines. In this particular case, the TVE-curves should not much differ from the plots of temperature dependence of electroconductivity in the Arrhenius coordinates. Almost precise quantitative coincidence of the plots is also due to that in the work under comparison,⁹⁴ the measurements were carried out in a reductive atmosphere (H_2 or $\text{H}_2+\text{H}_2\text{S}$), *i.e.*, under the conditions close to those of vacuum heating upon obtaining the TVE-curves. Note-worthy that the authors of the work discussed did not find in their measurements any general analytical opportunities and even paid no attention to that the method used reveals namely surface phases.

Deactivation and regeneration of catalysts

Destruction and reconstruction of an active surface solution (NiO — CuO —cement system in oxygen hydrogenation). Study of the performance of the NiO — CuO —aluminocalcium cement catalyst in the process of oxygen hydrogenation showed that in the case of significant overheating (to 800 °C), a specific surface structure was partially destructed (see p. 274) and the catalyst was deactivated.^{88,89} We proposed the procedure of regeneration without waste waters which includes the introduction of the additives of powder active oxide (or copper hydroxocarbonate, its precursor) in the deactivated catalyst followed by calcination at 250–300 °C resulting in the incorporation of the oxide into a surface solid solution by topochemical reaction.^{95,96} Complete regeneration proved to be achieved when adding 20 wt. % of Cu hydroxocarbonate in the catalyst. The surface phase analysis of the catalyst samples (Fig. 26) after deactivation (curve 2) and regeneration (curves 3–5) allowed one to identify a solid solution of CuO in the Al_2O_3 incorporated in a cement (curve 2 which is close to a band of cement). This means that in the deactivated catalyst the surface of the cement-based solid solution becomes uncovered because of sintering of the active surface solid solution of Al_2O_3 in CuO . After the regeneration of activity, the state of the surface (curves 4 and 5) approaches to that of the initial CuO -based solid solution (curve 1).

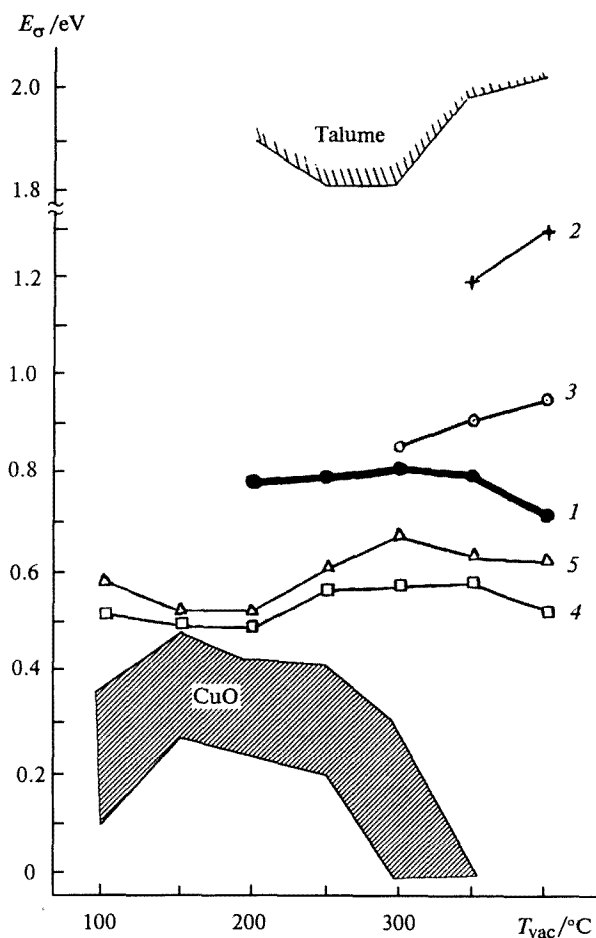


Fig. 26. Change in the electrical characteristics under deactivation and regeneration of the catalyst of the 20 CuO—15 NiO-cement (wt.%) composition in O_2 hydrogenation: 1, starting catalyst; 2, after deactivation; 3, after regeneration with calcination; 4, after regeneration with the addition of CuO ; 5, after regeneration with the addition of copper hydroxocarbonate.

Coke formation and refining of the surface (NiO —cement and NiO — CuO —cement systems in heavy oil residue cracking). The NiO — CuO —aluminocalcium cement system proved to be very perspective as the catalyst for cracking of heavy oil residue.⁹⁷ The analysis with the TVE-curves method made it possible to follow phase-structural state of the surface at all stages of this process. Figure 27 shows for the 35 mol. % NiO —cement catalyst that after the catalytic reaction, the surface is covered by coke film with a good conductivity (curve 2). The coke cannot be removed by gasification (curve 3). After regeneration (curve 4), the surface is purified from a coke but not return to the starting state, *i.e.*, to the NiO -based solid solution (curve 1), and proves to be irreversibly changed. Thus, the surface phase analysis shows that under conditions of the catalytic reaction, sintering of

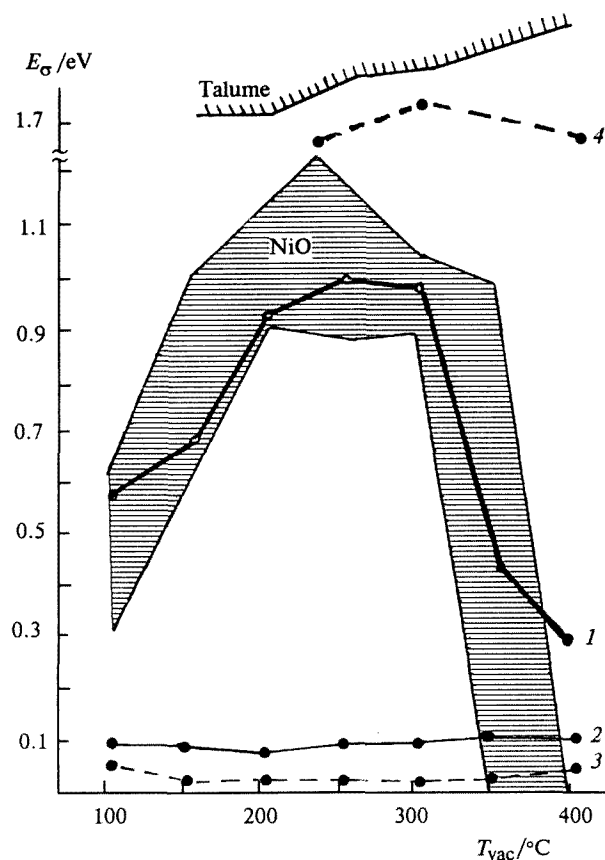


Fig. 27. Electrical characteristics of the catalyst of the 35 wt. % NiO—cement composition at various stages of heavy oil residue cracking: 1, starting catalyst; 2, after cracking; 3, after gasification; 4, after regeneration.

the active surface phase occurs (which is confirmed by the XRD data) and the cement-based solid solution of NiO in Al_2O_3 becomes uncovered (curve 4).

Systems with local control of electroconductivity

Ferrite structure. Comparison of the electrical behavior of ferrites of different composition revealed the peculiarity of the TVE-curves which is inherent, apparently, of all curves concerning to ferrite phases. Independently of chemical composition, the value of the activation energy of conductivity E_σ of ferrites in all range of T_{vac} is close to zero (see Fig. 22, curves 3 and 4). This is possibly connected with the mechanism of conductivity in ferrites which is based on the activationless exchange between $\text{Fe}^{2+} \leftrightarrow \text{Fe}^{3+}$ ions located at the neighboring B-positions of an elementary unit through all crystalline lattice. Similar mechanism can be realized not only in ferrites but in other systems containing ions with unstable valency (manganese, vanadium) as well as in the structures with interacting ions of transition and nontransition elements, e.g., in perovskites described in the following section.

Perovskite structure. The studies of past few years showed that complex oxides with perovskite structure (of ABO_3 summarized formula) exhibited catalytic activity in a number of reactions, which much depend not only on the composition of oxides but also on the distribution of cations between A- and B-positions of an elementary unit. By means of the TVE-curves, XRD, and XPS methods,⁹⁸ the effect on the catalytic activity in benzene hydrogenation of some A- and B-cations in synthesized perovskites of general formula $\text{A}_4[\text{BRe}_2\Box]\text{O}_{12}$, where A = Ba^{2+} , Sr^{2+} , B = Co^{2+} , Ni^{2+} , Ca^{2+} , \Box is a cationic vacancy, was studied. The surface phase analysis shows that the electronic state of the surface of perovskites of different composition is first due to the presence of Re^{7+} ions in B-positions, because the substitution of Co^{2+} ions located at the same positions for Ca^{2+} ions results in no essential difference in electrical behavior of oxides. The nature of cations in A-positions, Sr^{2+} or Ba^{2+} , also does not affect electroconductivity. Unlike Co^{2+} and Ca^{2+} , Ni^{2+} ions in B-positions hamper a current transfer. The Re^{7+} ions provide a semiconductor-type conductivity only in a perovskite structure whereas barium perrhenate proves to be a dielectric.

According to the XPS data, after the reaction of benzene hydrogenation at the surface of perovskites, ~25 mol. % of rhenium is reduced to Re^0 , but the conductivity remains of the semiconductor type. This means that rhenium metal does not form infinite percolative cluster. The perovskites studied differ significantly in catalytic activity: $\text{Sr}_4\text{CoRe}_2\Box\text{O}_{12}$ and $\text{Sr}_4\text{NiRe}_2\Box\text{O}_{12}$ are very active, but $\text{Sr}_4\text{CaRe}_2\Box\text{O}_{12}$ and $\text{Ba}_4\text{CoRe}_2\Box\text{O}_{12}$, as barium perrhenate, exhibit virtually no activity. At the same time, the differences between the TVE-curves for the perovskites of different composition are smoothed down after the catalytic reaction. Consequently, in the case of perovskites, the catalytic activity is first due to local properties of an active site. It was found that Sr in A-position provide the conditions for high activity, whereas Ba in A-position and Ca in B-position deactivate the catalyst.

One can conclude that the nature of the electroconductivity of perovskites and their catalytic activity are determined by the specificity of perovskite structure rather than chemical nature of the surface phase. In this structure, both the mechanism of conductivity and the activity are due to the presence of specific ions in special sites. It is because of a special mechanism of conductivity that in some compounds of perovskite structure, the conditions arise for appearance of high-temperature superconductivity (HTSC).

Anionic stabilization of a crystalline lattice

Surface phase analysis with the use of the TVE-curves method made it possible to establish that when the NiO—CuO system is prepared by coprecipitation by sodium carbonate from a solution of sulfates or by thermal decomposition of hydroxocarbonates, stabiliza-

tion of oxides obtained occurs toward heating in a vacuum (see Fig. 7, curve 7). This effect was explained by a phenomenon of modification of the crystalline lattice with residual anions (SO_4^{2-} , CO_3^{2-})⁹⁹ and referred to as the effect of anionic stabilization.⁶⁷

The observed stabilization of the $\text{NiO}-\text{CuO}$ solid solutions that were prepared from nitrates in the concentration region of 3–82 mol. % NiO (see Fig. 13) also seems to be due to the effect of anionic stabilization caused by high content of residual hydroxyls, which retain upon formation of solid solutions. The effect of anionic stabilization is also observed in a number of other systems studied, in particular, in the $\text{NiO}-\text{MoO}_3$ (see Fig. 16, curves 4 and 5) and $\text{ZnO}-\text{CuO}$ systems.¹⁰⁰

Possibilities and limitations of the method

On the basis of the results of the analysis performed and taking into account the examples considered, one can summarize the possibilities and efficiency of the use of the proposed method of the surface phase analysis.

The measurements of electroconductivity with a direct current, which are suitable in principle for characterization of disperse systems, have some peculiarities which are of a special interest for the study of catalysts. First, these measurements can probe the subsurface layers that determine the catalytic activity. Secondly, owing to the multiplicity of intergranular contacts and high value of the surface/bulk ratio that are inherent of powders, these measurements are extremely sensitive to surface processes and, hence, to genesis of a catalyst and changes in its surface.

The TVE-curves method allows one to carry out qualitative phase analysis of the surface of disperse systems. The content of a phase found at the surface can be evaluated only relatively on the basis of the difference in heights of the arrangement of the curves in a plot, *e.g.*, for a series of similar objects with different content of this phase (see Figs. 11, 13, and 15).

The developed method of the surface phase analysis is suitable mainly to the objects with a semiconductor conductivity, *viz.*, with the specific electroconductivity $\sigma_{20^\circ\text{C}}$ in the range from $10^{-2}-10^{-3}$ to $10^{-10}-10^{-12}$ $\text{Ohm}^{-1}\text{cm}^{-1}$. The TVE-curves do not reveal the qualitative differences neither among metals nor among dielectrics. However, this fact does not produce much limitations for the investigation of catalysts, because significant number of known catalitically active compounds and systems, *viz.*, nearly all oxides and sulfides, borides, carbides, many composite and supported catalysts, including metallic film structures, can be categorized as semiconductor objects.

The method can be used in two modifications: as the registration method for the analysis of some conditional-stationary state of the surface in the previously trained samples and as the method for controlling the processes of genesis in an *in situ* version, *i.e.*, for the samples which underwent no preliminary thermal treatment (see Figs.

21 and 22). As in both versions vacuum heating to 400°C causes commonly irreversible changes in the composition and structure of a sample, the TVE-curves obtained are, as a rule, irreversible, although at the initial stage of heating, when only desorption processes occur, at least a partial reversibility of the TVE-curve is possible.

The TVE-curves give information, as a rule, about predominant surface phase whose particles form a chain of continuous conducting contacts (an "infinite cluster") at the surface. However, under specific conditions, the possibility of detecting other phases also appears. 1. If the systems with changing components ratio rather than a separate sample of a fixed composition are under study, various surface phases are developed at different compositions (see Figs. 11, 13, 15, and 19). 2. If electronic switching occurs during vacuum heating, the left branch of the TVE-curve characterizes one phase and the right branch characterizes another phase (see Fig. 19, *a*, curves 2–4), or a break appears at the Arrhenius straight line at the specific temperature, and then the TVE-curve is divided to two branches, each of them determining its own phase (see Fig. 9, curve 4 and Fig. 22, curves 4 and 5). 3. If a phase transformation occurs. For example, upon reduction and sintering of supported active oxide, a support can become uncovered (see Fig. 26, curve 2 and Fig. 27, curve 4), while under thermolysis of a residual surface hydroxide an oxide can arise (see Fig. 7, curve 6). 4. In the case of overlapping (superposition) of the TVE-curves for two or several phases, one can observe the distortion of a curve and its shift in a plot (see Fig. 19, *b*, curves 1, 7). 5. When solid solutions form, the TVE-curve of a pure phase is shifted in a plot or somewhat distorted accepting an intermediate shape (see Fig. 19, *b*, curves 2–4 in comparison with curve 1).

Sensitivity of the method, determined as the lower limit of the concentration of a phase found, depends on the dispersion and distribution of phases in a system. Under statistical distribution, the concentration of 15–25 vol. % (a theoretical value of the percolation threshold) is necessary for the arising of conducting ("infinite") surface cluster. However, under the conditions favoring the determination (a thin layer on a support or the formation of a new phase at intergranular contacts), the sensitivity can achieve 1 %, *i.e.*, to exceed substantially that of the XRD method, as was shown for the $\text{NiO}-\text{TiO}_2$ system (see Fig. 15). On the other hand, one can judge about the character of phase distribution in an object by the difference in the sensitivity for specific phases. For example, insensitivity to the presence of nickel metal in the reduced $\text{NiO}-\text{TiO}_2$ system (see Fig. 17) gives evidence for the screening of the metal particles by a support.

In the combination with other physical and physico-chemical methods (XRD, XPS, electron microscopy, adsorption, catalytic test reactions), the TVE-curves method allows one to obtain a new information about phase-structural state of an object, genesis and transformations of catalitically active surface, in particular,

about the appearance, distribution, migration, and interaction of surface phases.

Conclusions

The method of thermovacuum curves of electroconductivity (the TVE-curves method) makes it possible to carry out qualitative estimation of the phases at the surface of a disperse object by measuring the electroconductivity with a direct current during heating *in vacuo*. The method is very simple; nevertheless, it helps to obtain new and uncommon information in many cases. In combination with other physical measurements, the proposed method allows one for the first time to characterize at the phase level the surface of various catalytic systems of semiconductor type (single, complex, and supported oxides, sulfides, chlorides). With the use of the method, one manages to follow the biography of an active surface starting from the precursors of active phases and to compare the catalytic activity of the objects studied with the surface phase composition. The use of the TVE-curves method contributed much to solving a number of problems of heterogeneous catalysis related to the genesis and state of an active surface, as well as deactivation and regeneration of a catalyst. First, these include problems on the formation of surface solid solutions, migration and distribution of surface phases the relation between catalytic activity and the surface phase structural state, the mechanism of interaction of an active phase with a support, and the conditions of stabilization, destruction, and regeneration of active structures. The TVE-curves method, in combination with the procedures of "electroconductivity—composition" and percolation analysis, allows one to extend the possibilities of these procedures owing to the identification of the phases revealed.

The applications of the TVE-curves method are prospective not only in the field of heterogeneous catalysis but also for solving problems connected with other disperse solids: adsorbents, ceramics, sensors, HTSC-materials, organic semiconductors,^{101,102} as well as of problems of topochemistry⁸⁵ and mechanochemistry.¹⁰³

The authors are grateful to the ISF and RFBR for assistance that provided the opportunity to significantly develop the computer simulation of catalysts and on this basis to prepare a special part of this review as well as to carry out more profound analysis of all reviewed data.

This work was financially supported by the International Science Foundation (Grants M63 000 and M63 300) and by the Russian Foundation for Basic Research (Project No. 95-03-08606a).

References

1. *Spectroscopic Characterization of Heterogeneous Catalysts. Studies in Surface Science and Catalysis*, **57 A,B**, Ed. J. L. G. Fierro, Elsevier, 1990, 385.
2. B. T. Kolomiets, I. T. Sheftel', and E. V. Kurlina, *Zh. Tekh. Fiz. [J. Tech. Phys. USSR]*, 1957, **27**, 51 (in Russian).
3. E. M. Shvarts, V. V. Grundstein, and A. F. Levin'sh, *Izv. Akad. Nauk Latv. SSR, Ser. Khim.*, [Bull. Acad. Sci. Latv. SSR, Div. Chem. Sci.], 1968, 259 (in Russian).
4. B. Gillot, J. F. Ferriot, and A. Rousset, *J. Phys. Chem. Solids*, 1976, **37**, 857.
5. B. Gillot and A. Rousset, *C. R. Acad. Sci.*, 1981, **293**, 23.
6. O. Popa, P. Rotaru, S. I. Blejoiu, L. Pandele, O. Binescu, I. Brasoveanu, and D. I. Marchidan, *Rev. Roum. Chim.*, 1979, **24**, 153.
7. G. Gray, in *Experimental Methods in Catalytic Research*, Academic Press, New York—London, 1969, 480 p.
8. F. F. Volksenstejn, *Elektronnaya teoriya kataliza na poluprovodnikakh* [Electronic Theory of Catalysis on Semiconductors], Fizmatgiz, Moscow, 1960, 187 p. (in Russian).
9. *Elektronnaya yavleniya v adsorbsii i katalize na poluprovodnikakh* [Electronic Phenomena in Adsorption and Catalysis on Semiconductors], Mir, Moscow, 1969, 389 p. (in Russian).
10. V. F. Kiselev and O. V. Krylov, *Elektronnaya yavleniya v adsorbsii i katalize na poluprovodnikakh i dielektrikakh* [Electronic Phenomena in Adsorption and Catalysis on Semiconductors and Dielectrics], Nauka, Moscow, 1973, 400 p. (in Russian).
11. F. F. Volksenstejn, *Fiziko-khimiya poverkhnosti poluprovodnikov* [Physicochemistry of the Surface of Semiconductors], Nauka, Moscow, 1973, 400 p. (in Russian).
12. R. Kumar, B. L. Bishwas, B. Kumar, J. N. Tiwari, and S. Bhagat, *J. Indian Chem. Soc.*, 1989, **66**, 746.
13. I. V. Nicolescu, Gh. Nedelcu, and A. Szabo, *Rev. Roum. Chim.*, 1990, **35**, 185.
14. R. M. Gabr, A. M. El-Awad, and M. M. Girdis, *Mat. Chem. Phys.*, 1991, **30**, 69.
15. C. Yu, W. Li, W. Feng, A. Ai, and Y. Chen, *Proc. Internat. Congress Catal.*, Elsevier, Budapest, 1992, 1119.
16. A. A. Said, *Collect. Czech. Chem. Commun.*, 1993, **58**, 1591.
17. F. Rouvet, J.-M. Herrmann, and J.-C. Volta, *J. Chem. Soc., Faraday Trans.*, 1994, **90**, 1441.
18. A. A. Dulov and L. A. Abramova, *Vozmozhnosti metoda elektroprovodnosti v issledovaniyakh katalizatorov*, Itogi Nauki Tekh., Ser. Kinet. Katal., [Possibilities of the Method of Electroconductivity in the Study of Catalysts], 1984, **12**, 144 (in Russian).
19. *Problemy fiziki poluprovodnikov* [Problems of the Physics of Semiconductors], Izd-vo inostr. lit., Moscow, 1957, 345; C. G. B. Garrett and W. H. Brattain, *Phys. Rev.*, 1955, **99**, 376.
20. J. C. Slater, *Phys. Rev.*, 1956, **103**, 1631.
21. R. L. Petritz, *Phys. Rev.*, 1956, **104**, 1508.
22. B. I. Shklovskii, *Fizika i tekhnika poluprovodnikov* [Physics and Engineering of Semiconductors], 1979, **13**, 93 (in Russian).
23. A. Ya. Vinnikov, A. M. Meshkov, and V. N. Savushkin, *Fizika tverdogo tela* [Phys. of Solids], 1980, **22**, 2989; 1985, **27**, 1929, (in Russian).
24. L. I. Burbulyavichus, Yu. A. Zarifants, V. F. Kiselev, and S. V. Khrustaleva, *Kinet. Katal.*, 1971, **12**, 922 [*Kinet. Catal.*, 1971, **12** (Engl. Transl.)].
25. G. M. Kozub, A. M. Turchaninov, I. G. Voroshilov, and V. L. Chernobravets, *Teor. Eksp. Khim.*, 1975, **11**, 560 [*Theor. Exp. Chem.*, 1975, **11** (Engl. Transl.)].
26. V. Ya. Sukharev, V. V. Chistyakov, and I. A. Myashikov, *J. Phys. Chem. Solids*, 1988, **49**, 333.
27. V. Ya. Sukharev, *J. Chem. Soc., Faraday Trans.*, 1993, **89**, 559.

28. L. A. Abramova, S. P. Baranov, and A. A. Dulov, *Izv. Akad. Nauk, Ser. Khim.*, 1993, 1868 [Russ. Chem. Bull., 1993, **42**, 1782 (Engl. Transl.)].

29. L. A. Abramova, A. A. Dulov, and S. P. Baranov, *J. Phys. Chem. Solids*, 1994, **55**, 367; L. A. Abramova, S. P. Baranov, and A. A. Dulov, *Mendeleev Commun.*, 1995, 150; L. A. Abramova, S. P. Baranov, and A. A. Dulov, *Izv. Akad. Nauk, Ser. Khim.*, 1995, 1449 [Russ. Chem. Bull., 1995, **44**, 1391 (Engl. Transl.)].

30. S. Kirkpatrick, *Rev. Mod. Phys.*, 1973, **45**, 547.

31. B. I. Shklovskii and A. L. Efros, *Elektronnye svoistva legirovannykh poluprovodnikov* [Electronic Properties of Doped Semiconductors], Nauka, Moscow, 1979, 416 p. (in Russian).

32. A. Ya. Vinnikov, *Zh. Eksp. Teor. Fiz. [J. Exp. Theor. Phys.]*, 1989, **96**, 299 (in Russian).

33. F. Clément, P. Leroux-Hugon, and P. Argyrakis, *Phys. Rev. E*, 1994, **49**, 4857.

34. L. A. Abramova, S. P. Baranov, and A. A. Dulov, *Izv. Akad. Nauk, Ser. Khim.*, 1993, 1874 [Russ. Chem. Bull., 1993, **42**, 1788 (Engl. Transl.)].

35. L. A. Abramova, A. A. Dulov, and S. P. Baranov, *J. Phys. Chem. Solids*, 1994, **55**, 373.

36. K. Hauffe, *Reaktionen in und an Festen Stoffen*, v. 1, Springer Verlag, Berlin, 1966, 460 p.

37. E. J. W. Verwey, *Bull. Soc. Chim. Fr.*, 1949, D122.

38. V. N. Eremenko and A. M. Beinish, *Zh. Neorg. Khim.*, 1956, **1**, 2118 [*J. Inorg. Chem. USSR*, 1956, **1** (Engl. Transl.)].

39. L. N. Kurina and O. N. Ediseeva, *Kinet. Katal.*, 1973, **14**, 267 [*Kinet. Catal.*, 1973, **14** (Engl. Transl.)].

40. Yu. F. Kargin, V. A. Kutvitskii, and V. M. Skorikov, *Izv. Akad. Nauk SSSR, Ser. Neorg. Mater.*, 1977, **13**, 128 [*Inorg. Mater.*, 1977, **13** (Engl. Transl.)].

41. A. A. Kabanov, *Usp. Khim.*, 1971, **40**, 2029 [Russ. Chem. Rev., 1971, **40** (Engl. Transl.)].

42. A. A. Kabanov, *Zh. Fiz. Khim.*, 1979, **53**, 817 [Russ. J. Phys. Chem., 1979, **53** (Engl. Transl.)].

43. Z. Solo, M. Trojan, and M. Kuchler, *Thermochim. Acta*, 1985, **92**, 425.

44. J. Dereń and J. Haber, *J. Electrochem. Soc.*, 1966, **113**, 1349.

45. R. B. Bjorklund and I. Lundström, *J. Catal.*, 1983, **79**, 314.

46. A. Wilson and J. D. Wright, *Mol. Cryst. Liq. Cryst.*, 1992, **211**, 321.

47. F. Solymosi and L. Gera, *J. Phys. Chem.*, 1971, **75**, 491.

48. G. Sengupta, R. Chatterjee, P. K. Hazra, B. Chakraborty, R. Prasad, R. K. Sharma, and S. P. Sen, *Technology (India)*, 1975, **12**, 162.

49. R. B. Bjorklund, D. Soderberg, and I. Lundström, *J. Chem. Soc., Faraday Trans. 1*, 1985, **81**, 1715.

50. A. A. Slinkin and L. V. Ermolov, *Usp. Khim.*, 1991, **60**, 689 [Russ. Chem. Rev., 1991, **60** (Engl. Transl.)].

51. J.-M. Herrmann and P. Pichat, *J. Catal.*, 1982, **78**, 425.

52. B. H. Chen and J. M. White, *J. Phys. Chem.*, 1982, **86**, 3534.

53. C. Yixuan, W. Zhaobin, C. Yanxin, L. Huaxin, H. Zupei, L. Huiqung, D. Yonglei, Y. Chunying, and L. Wenzhao, *J. Mol. Catal.*, 1983, **21**, 275.

54. C. R. F. Lund and J. A. Dumesic, *J. Phys. Chem.*, 1982, **86**, 130.

55. R. L. Chin and D. M. Hercules, *J. Phys. Chem.*, 1982, **86**, 360.

56. A. A. Dulov, L. A. Abramova, D. P. Shashkin, and A. M. Rubinshtein, *Kinet. Katal.*, 1972, **13**, 180 [*Kinet. Catal.*, 1972, **13** (Engl. Transl.)].

57. A. M. Rubinstein, A. A. Dulov, A. A. Slinkin, L. A. Abramova, I. Sh. Gershenson, L. A. Gorskaya, V. Ja. Danyushevskii, M. I. Dashevskii, A. L. Klyachko-Gurvich, T. K. Lavrovskaya, L. I. Lafer, and V. I. Yakerson, *J. Catal.*, 1974, **235**, 80.

58. A. A. Slinkin, T. K. Lavrovskaya, A. A. Dulov, L. A. Abramova, and A. M. Rubinstein, *Tezisy dokl. Vsesoyuzn. konf. po mekhanizmu geterogennykh kataliticheskikh reaktsii* [Abstr. of Papers, All-Union Conference on the Mechanism of Heterogeneous Catalytic Reactions], Moscow, 1974, 50 (in Russian).

59. A. A. Dulov, L. A. Abramova, V. I. Yakerson, E. Z. Golosman, V. I. Artamonov, and A. M. Rubinshtein, *Kinet. Katal.*, 1979, **20**, 937 [*Kinet. Catal.*, 1979, **20** (Engl. Transl.)].

60. A. A. Dulov, L. A. Abramova, and A. M. Rubinshtein, *Kinet. Katal.*, 1979, **20**, 931 [*Kinet. Catal.*, 1979, **20** (Engl. Transl.)].

61. A. A. Dulov and L. A. Abramova, *Catalyse et Environnement, 7-eme Colloque Franco-sovietique de Catalyse*, Strasbourg, 1987, 134.

62. F. J. Gil-Llambias and A. M. Escudey-Castro, *J. Chem. Soc., Chem. Commun.*, 1982, 478.

63. J. Petro, T. Mallat, S. Szabo, and F. Hange, *J. Electroanal. Chem.*, 1984, **160**, 289.

64. J. Gal, S. Kamoun, J. Perichon, Liang Tse Yu, J. Barrault, and C. Renard, *Cl Mol. Chem.*, 1985, **1**, 325.

65. S. Subramanian, J. S. Noh, and J. A. Schwarz, *J. Catal.*, 1988, **114**, 433.

66. G. Binnig and H. Rohrer, *IBM J. Res. Dev.*, 1986, **30**, 355.

67. A. A. Dulov, L. A. Abramova, and I. Sh. Gershenson, *Kinet. Katal.*, 1990, **31**, 1510 [*Kinet. Catal.*, 1990, **31** (Engl. Transl.)].

68. A. A. Dulov, L. A. Abramova, A. A. Slinkin, A. L. Klyachko, M. I. Dashevskii, G. A. Ashavskaya, L. I. Lafer, V. I. Yakerson, and A. M. Rubinshtein, *Izv. Akad. Nauk SSSR, Ser. Khim.*, 1976, 265 [*Bull. Acad. Sci. USSR, Div. Chem. Sci.*, 1976, **25** (Engl. Transl.)].

69. A. A. Dulov, A. A. Slinkin, L. A. Abramova, I. Sh. Gershenson, E. A. Fedorovskaya, and A. M. Rubinshtein, *Izv. Akad. Nauk SSSR, Ser. Khim.*, 1984, 979 [*Bull. Acad. Sci. USSR, Div. Chem. Sci.*, 1984, **33**, 900 (Engl. Transl.)].

70. A. A. Dulov, T. K. Lavrovskaya, A. A. Slinkin, and A. M. Rubinshtein, *Izv. Akad. Nauk SSSR, Ser. Khim.*, 1984, 986 [*Bull. Acad. Sci. USSR, Div. Chem. Sci.*, 1984, **33**, 907 (Engl. Transl.)].

71. A. A. Dulov, L. A. Abramova, T. K. Lavrovskaya, A. A. Slinkin, G. A. Ashavskaya, and A. M. Rubinshtein, *Tezisy dokl. IV Vsesoyuzn. konf. po mekhanizmu kataliticheskikh reaktsii* [Abstr. of Papers, IV All-Union Conference on the Mechanism of Catalytic Reactions], Moscow, 1986, Pt. 2, 269 (in Russian).

72. A. A. Dulov, L. A. Abramova, T. K. Lavrovskaya, and G. A. Ashavskaya, *Tezisy dokl. na IX Vsesoyuzn. soveshchanii po kinetike i mekhanizmu khimicheskikh reaktsii v tverdom tele, Alma-Ata*, 1986 [Abstracts of Papers, IX All-Union Workshop on Kinetics and Mechanism of Chemical Reactions in a Solid], Chernogolovka, 1986, 17 (in Russian).

73. A. A. Dulov, L. A. Abramova, E. Z. Golosman, V. N. Efremov, and V. I. Yakerson, *Kinet. Katal.*, 1988, **29**, 749 [*Kinet. Catal.*, 1988, **29** (Engl. Transl.)].

74. A. A. Dulov, M. I. Dashevskii, A. L. Klyachko-Gurvich, A. A. Slinkin, and A. M. Rubinshtein, *Izv. Akad. Nauk SSSR, Ser. Khim.*, 1972, 2156 [*Bull. Acad. Sci. USSR, Div. Chem. Sci.*, 1972, **21**, 2094 (Engl. Transl.)].

75. A. M. Rubinshtein, A. A. Dulov, V. I. Yakerson, L. A.

Gorskaya, and L. A. Abramova, *Izv. Akad. Nauk SSSR, Ser. Khim.*, 1974, 1645 [*Bull. Acad. Sci. USSR, Div. Chem. Sci.*, 1974, **23** (Engl. Transl.)].

76. M. I. Dashevskii, A. A. Dulov, V. I. Yakerson, A. L. Klyachko-Gurvich, and A. M. Rubinshtein, *Tezisy dokl. IX Vsesoyuzn. konf. po elektronnoi mikroskopii, Tbilisi* [Abstr. of Papers, IX All-Union Conf. on Electron Microscopy, Tbilisi], Nauka, Moscow, 1973, 17 (in Russian).

77. Jae Shi Choi and Keu Hong Kim, *J. Phys. Chem.*, 1976, **80**, 666.

78. A. A. Dulov, L. A. Abramova, I. Sh. Gershenzon, and A. M. Rubinshtein, *Dokl. Akad. Nauk SSSR*, 1973, **210**, 345 [*Dokl. Chem.*, 1973, **210** (Engl. Transl.)].

79. A. A. Dulov, I. Sh. Gershenzon, and A. M. Rubinshtein, *Kinet. Katal.*, 1974, **15**, 197 [*Kinet. Catal.*, 1974, **15** (Engl. Transl.)].

80. A. A. Slinkin, E. A. Fedorovskaya, L. A. Abramova, T. N. Kucherova, T. K. Lavrovskaya, and A. A. Dulov, *Kinet. Katal.*, 1984, **25**, 436 [*Kinet. Catal.*, 1984, **25** (Engl. Transl.)].

81. A. A. Dulov, L. A. Abramova, T. N. Kucherova, and A. A. Slinkin, *Kinet. Katal.*, 1984, **25**, 1432 [*Kinet. Catal.*, 1984, **25** (Engl. Transl.)].

82. A. A. Slinkin, A. A. Dulov, E. S. Shpiro, L. V. Ermolov, L. A. Abramova, A. Yu. Stakheev, and T. N. Kucherova, *Kinet. Katal.*, 1988, **29**, 694 [*Kinet. Catal.*, 1988, **29** (Engl. Transl.)].

83. N. M. D. Brown, J. B. McMonagle, and G. N. Greaves, *J. Chem. Soc., Faraday Trans. I*, 1984, **80**, 589.

84. A. A. Dulov, L. A. Abramova, S. S. Goryashchenko, and K. I. Slovetskaya, *Kinet. Katal.*, 1990, **31**, 1258 [*Kinet. Catal.*, 1990, **31** (Engl. Transl.)].

85. A. A. Dulov and L. A. Abramova, *Tezisy dokl. X Vsesoyuzn. soveshch. po kinetike i mekhanizmu khimich. reaktsii v tverdom tele, Chernogolovka* [Abstr. of Papers, X All-Union Workshop on Kinetics and Mechanism of Chemical Reactions in a Solid], Moscow, 1989, **1**, 36.

86. A. A. Dulov, L. A. Abramova, E. Z. Golosman, and V. I. Yakerson, *Kinet. Katal.*, 1990, **31**, 186 [*Kinet. Catal.*, 1990, **31** (Engl. Transl.)].

87. A. A. Dulov, E. M. Stasenko, V. N. Efremov, G. M. Tesakova, L. A. Abramova, E. Z. Golosman, and V. I. Yakerson, *Kinet. Katal.*, 1992, **33**, 411 [*Kinet. Catal.*, 1992, **33** (Engl. Transl.)].

88. A. A. Dulov, E. M. Stasenko, L. A. Abramova, S. V. Karamanenko, I. A. Mamaeva, E. Z. Golosman, and V. I. Yakerson, *Kinet. Katal.*, 1992, **33**, 1183 [*Kinet. Catal.*, 1992, **33** (Engl. Transl.)].

89. A. A. Dulov, B. N. Kuznetsov, E. M. Stasenko, and V. I. Yakerson, *Kinet. Katal.*, 1993, **34**, 362 [*Kinet. Catal.*, 1993, **34** (Engl. Transl.)].

90. A. A. Dulov, L. A. Abramova, G. I. Frankfurt, E. Z. Golosman, A. L. Lapidus, S. D. Sominskii, and V. I. Yakerson, *Izv. Akad. Nauk SSSR, Ser. Khim.*, 1987, 1724 [*Bull. Acad. Sci. USSR, Div. Chem. Sci.*, 1987, **36**, 1594 (Engl. Transl.)].

91. I. G. Solomonik, A. A. Dulov, L. A. Abramova, I. I. Kurlyandskaya, and V. I. Yakerson, *Tezisy dokl. I Vsesoyuzn. konf. po katalizu i kataliticheskim protsessam proizvodstva khimiko-farmatsevicheskikh preparatov* [Abstr. of Papers, I All-Union Conf. on Catalysis and Catalytic Processes in the Production of Chemical-Pharmaceutical Preparations], Moscow, 1985, Pt. 1, 76 (in Russian).

92. A. A. Dulov, L. A. Abramova, E. N. Amirkov, F. V. Aliev, and A. M. Rubinshtein, *Kinet. Katal.*, 1983, **24**, 413 [*Kinet. Catal.*, 1983, **24** (Engl. Transl.)].

93. A. A. Dulov, L. A. Abramova, S. I. Kondrat'ev, S. B. Nikishenko, G. V. Antoshin, and Kh. M. Minachev, *Kinet. Katal.*, 1985, **26**, 1510 [*Kinet. Catal.*, 1985, **26** (Engl. Transl.)].

94. M. Breysse, R. Fréty, M. Vrinat, P. Grange, and M. Genet, *Appl. Catal.*, 1984, **12**, 165.

95. A. A. Dulov, L. A. Abramova, E. M. Stasenko, E. Z. Golosman, and V. I. Yakerson, *Tezisy dokl. Vsesoyuzn. nauchno-tehnicheskoi konf. "Ekologiya khimicheskikh protzvodstv"* [Abstr. of Papers, All-Union Scientific-Engineering Conference "Ecology of Chemical Production"], Severodonetsk, 1990, 211 (in Russian).

96. A. A. Dulov, L. A. Abramova, E. M. Stasenko, V. N. Efremov, G. M. Tesakova, E. Z. Golosman, and V. I. Yakerson, *Izv. Akad. Nauk, Ser. Khim.*, 1994, 1559 [*Russ. Chem. Bull.*, 1994, **43**, 1471 (Engl. Transl.)].

97. A. A. Dulov, E. M. Stasenko, L. A. Abramova, R. B. Akhverdiev, G. A. Ashavskaya, E. Z. Golosman, and V. I. Yakerson, *Kinet. Katal.*, 1995, **36** [*Kinet. Catal.*, 1995, **36** (Engl. Transl.)].

98. M. A. Ryashentseva, A. A. Dulov, L. A. Abramova, O. P. Tkachenko, V. V. Fomichev, and A. E. Vetrov, *J. Catal.*, 1990, **125**, 1.

99. T. M. Yur'eva, *Kinet. Katal.*, 1985, **26**, 686 [*Kinet. Catal.*, 1985, **26** (Engl. Transl.)].

100. A. A. Dulov, L. A. Abramova, E. Z. Golosman, and V. I. Yakerson, *Mezvuzovskii sb. nauch. trudov* [Intercollegiate Collection of Scientific Works], Ivanovo, 1986, 49 (in Russian).

101. A. A. Dulov, L. A. Abramova, A. I. Sherle, and V. R. Epshtein, in *Elektronika organicheskikh materialov* [Electronics of Organic Materials], Nauka, Moscow, 1985, 242 (in Russian).

102. B. A. Snovok, Ya. D. Lampeka, and M. V. Kurik, *Fizika tverdogo tela* [Phys. of Solids], 1994, **36**, 2881 (in Russian).

103. L. A. Abramova and A. A. Dulov, *Tezisy dokl. nauchno-tehnich. seminara "Mekhanokhimiya i mekanich. aktivatsiya"* [Abstr. of Papers, Scientific-Engineering Seminar "Mechanochemistry and Mechanical Activation"], Saint-Petersburg, 1995, 48 (in Russian).